Establishment of a reverse genetic system and determination of the responsible gene for the enhanced virulence of trisegmented bunyaviruses

3 分節ゲノムを有するブニヤウイルスを対象としたリバースジェネティクス系の確立および病原性に関与するウイルス遺伝子の特定

Joint Graduate School of Veterinary Medicine
Yamaguchi University

Shelly Wulandari

March 2025

Establishment of a reverse genetic system and determination of the responsible gene for the enhanced virulence of trisegmented bunyaviruses

3 分節ゲノムを有するブニヤウイルスを対象としたリバースジェネティクス系の確立および病原性に関与するウイルス遺伝子の特定

ACADEMIC DISSERTATION

Presented to

Joint Graduate School of Veterinary Medicine

Yamaguchi University, Japan

By

Shelly Wulandari

Laboratory of Veterinary Microbiology

Joint Faculty of Veterinary Medicine,

Yamaguchi University, Japan

In partial fulfillment of requirements for the degree of

Doctor of Philosophy

In

Veterinary Medicine

March 2025

JOINT GRADUATE SCHOOL OF VETERINARY MEDICINE
YAMAGUCHI UNIVERSITY

We hereby recommend that the thesis prepared under supervision by Shelly Wulandari, entitled "Establishment of a Reverse Genetic System and Determination of the Responsible Gene for the Enhanced Virulence of Trisegmented Bunyaviruses" should be accepted as fulfilling in part for the degree of Doctor of Philosophy.

Committee in Graduate Work:

Daisuke HAYASAKA, DVM., Ph.D
Chairperson of supervisory committee

Takuya MIZUNO, DVM., Ph.D
Co-Supervisor

Hiroshi SHIMODA, DVM., Ph.D
Co-Supervisor

Ai TAKANO, DVM., Ph.D
Co-Supervisor

Yusuke MATSUMOTO, DVM., Ph.D
Co-Supervisor

Table of contents

List of Tables

List of Figures

Definitions/Abbreviations

Abbreviation	Definition
BSL	Biosafety level
BUNV	Bunyamwera virus
CCHF	Crimean–Congo haemorrhagic fever
CCHFV	Crimean–Congo haemorrhagic fever virus
cDNA	Complementary DNA
CPE	Cytopathic effect
cRNA	Complementary RNA
DAB	3,3'-diaminobenzidine tetrahydrochloride
DMEM	Dulbecco's modified Eagle's minimum essential medium
DPI	Days post-infection
FBS	Fetal bovine serum
FFA	Focus forming assay
FFA	Focus forming-assay
FFU	Focus-forming units
Gc	Glycoprotein C
GFP	Green fluorescent protein
Gn	Glycoprotein N
GP	Glycoprotein
GPC	Glycoprotein precursor
HAZV	Hazara virus
HDVr	Hepatitis delta virus ribozyme
HPI	Hours post-infection
HRTV	Heartland bandavirus
HTNV	Hantaan virus
ICTV	International Committee on Taxonomy of Viruses
IFN-I	Type I interferon
IFNAR	Type I interferon recoptor
IRES	Encephalomyocarditis virus internal ribosome entry site sequence
LACV	LaCrosse virus

MOI	Multiplicity of infection
mRNA	Messenger RNA
NP	Nucleocapsid protein
NSDV	Nairobi sheep disease virus
NSm	Medium non-structural protein
NSs	Non-structural S protein
OPTI-MEM	Opti-minimum essential media
ORF	Open reading frame
OROV	Oropouche virus
PCR	Polymerase chain reaction
PDB	Protein data bank
Pol I	Polymerase I
qRT-PCR	Quantitative reverse transcription polymerase chain reaction
RdRp	RNA-dependent RNA polymerase
RNP	Ribonucleoprotein complex
RVFV	Rift valley fever virus
SBV	Schmallenberg virus
SC	Subcutaneous
SFTS	Severe fever with thrombocytopenia syndrome
SFTSV	Severe fever with thrombocytopenia syndrome virus
STAT2	Signal transducer and activator of transcription 2
T7 Pol	T7 Polymerase
TFLV	Tofla Virus
UTR	Untranslated region
vRNA	Viral RNA
WELV	Wetland virus
YEZV	Yezo virus

1. General Introduction

1.1 Introduction

Trisegmented bunyaviruses constitute a category of viruses within the *Bunyavirales* order, distinguished by their segmented, negative-sense RNA genomes that are encoded in an orientation opposite to that of messenger RNA. Their members infect broad ranges of hosts, including several significant human pathogens, such as severe fever with thrombocytopenia syndrome virus (SFTSV), Hantaan virus (HTNV), Crimean-Congo hemorrhagic fever virus (CCHFV), Bunyamwera virus (BUNV), and Rift Valley fever virus (RVFV) (Ren et al., 2021). The genome segments are labeled as L, M, and S, where the L segment encodes the RNA-dependent RNA polymerase, the M segment encodes glycoproteins, and the S segment encodes nucleoproteins and nonstructural proteins (Tercero and Makino, 2020; Hartman and Myler, 2023).

Reverse genetic systems have been essential in the investigation of trisegmented bunyaviruses. The process of introducing a precise genetic change into a viral genome, known as viral reverse genetics, has revolutionized our understanding of negative-sense, segmented RNA viruses. While the specific characteristics of reverse genetic systems vary among different viruses, the fundamental principles of biology remain the same. Firstly, we reverse transcribe and clone the full-length RNA viral genome into DNA plasmids for *in vitro* manipulation. We then introduce the genome-encoding plasmids into cells, usually in conjunction with helper protein expression plasmids, to produce the recombinant virus. These systems allow for the manipulation of viral genomes to study virus biology and pathogenesis. The development of these systems involves generating viral transcripts from transfected plasmids, which can then be used to produce recombinant viruses.

Numerous bunyaviruses are highly pathogenic, requiring biosafety level 3 or 4 facilities for handling. This restricts the scope of research and development activities that

can be conducted safely. In this study, we were able to rescue recombinant Tofla virus (TFLV) and SFTSV from cDNA clones, allowing detailed studies on viral genetics and pathogenesis. We also describe the molecular determinants of virulence in SFTSV, which is crucial for developing effective vaccines and therapeutics. Finally, we highlight that reverse genetics continues to be a powerful tool in elucidating the molecular mechanisms of virulence in trisegmented bunyaviruses, which will contribute to our understanding of viral biology, pathogenesis, and intervention strategies.

1.2 Bunyaviruses

Bunyaviruses are member of the order *Bunyavirales,* represent the largest group of RNA viruses and are responsible for numerous fever and hemorrhagic diseases. Originally discovered in 1943 in Uganda (Smithburn et al., 1946), the Bunyaviridae family has grown to include over 500 named virus species found worldwide (Boshra, 2022). Primarily, arthropod and rodent vectors transmit these predominantly tri-segmented, single-stranded RNA viruses, which can infect a wide variety of animals and plants (Horne & Vanlandingham, 2014). Despite only encoding a small number of proteins, these viruses have the ability to cause potentially fatal disease outcomes and have even developed strategies to suppress the innate antiviral immune mechanisms of the infected host.

1.2.1 Classification

The International Committee on Taxonomy of Viruses (ICTV) has made several updates to the taxonomy of bunyaviruses in recent years. In 2017, ICTV established the order *Bunyavirales*, which is short for "Bunyaviruses." This order is used to group together viruses that have segmented, linear, single-stranded, negative-sense, or

ambisense RNA genomes. Subsequent taxonomic updates further developed this order, which now comprises 14 families. These families include *Arenaviridae, Cruliviridae, Fimoviridae, Hantaviridae, Leishbuviridae, Mypoviridae, Nairoviridae, Peribunyaviridae, Phasmaviridae, Phenuiviridae, Tospoviridae,* and *Wupedeviridae.* In 2019, the ICTV added two additional families, *Leishbuviridae* and *Tospoviridae* (Abudurexiti et al., 2019). The ICTV continues to update the taxonomy of Bunyavirales as new viruses are discovered and classified, reflecting the ongoing research and understanding of this diverse viral order.

Several bunyaviruses have attracted significant attention for research due to their impact on human health and economic consequences. Severe Fever with Thrombocytopenia Syndrome Virus (SFTSV), this newly discovered tick-borne bunyavirus, has gained attention due to its high mortality rate of over 40% (Ye & Yan, 2024). Crimean-Congo hemorrhagic fever (CCHF) is a severe tick-borne illness with a wide geographical distribution and case fatality rates of 30% or higher. Infection with the CCHF virus (CCHFV) causes the illness, with cases reported throughout Africa, the Middle East, Asia, and southern and eastern Europe. The expanding range of the Hyalomma tick vector is placing new populations at risk for CCHF, and no licensed vaccines or specific antivirals exist to treat it (Hawman & Feldmann, 2023).

The family *Arenaviridae, Hantaviridae, Peribunyaviridae,* and *Phenuiviridae* also contains a variety of commonly known typical pathogenic viruses, including the lymphocytic choriomeningitis virus (LCMV, *Arenaviridae* family), known to cause fetal developmental defects (Barton et al., 2002). Hantaan virus (HTNV, *Hantaviridae* family) is mainly distributed in Europe and Asia (Brocato and Hooper, 2019). The *Peribunyaviridae* family members La Crosse Virus (LACV), Schmallenberg Virus (SBV), and Oropouche Virus (OROV) have demonstrated the ability to transcend species

barriers and impact human health (Hulswit et al., 2021), while the Rift Valley fever virus (RVFV, *Phenuiviridae* family) poses a significant threat to both human health and livestock biosecurity (Linthicum et al., 2016). Thus, research on bunyaviruses continues to expand our understanding of their molecular biology, pathogenesis, and potential control strategies.

1.2.2 Structure

Bunyaviruses have a tripartite genome consisting of three single-stranded RNA segments: large (L), medium (M), and small (S). The genome segments are organized as follows: The L segment encodes the RNA-dependent RNA polymerase. The M segment encodes a polyprotein precursor, which undergoes processing into glycoprotein Gn (32–35 kDa), glycoprotein Gc (110–120 kDa), and non-structural protein NSm (found in some bunyaviruses). The S segment encodes nucleocapsid protein (N) and non-structural protein NSs (in most orthobunyaviruses) (Elliott, 2014).

Each genome segment contains untranslated regions (UTRs) at both 5' and 3' ends, which are important for transcription, replication, and genome encapsidation. The terminal nucleotides of each segment are complementary, forming a "panhandle" structure that serves as the promoter for transcription and replication (Elliott, 2014).

1.2.3 Replication cycle within the mammalian host

The three segments of the bunyavirus genome (L, M, and S) interact in several ways during replication. Complementary terminal sequences: The 3' and 5' termini of each genome segment are highly conserved and complementary, allowing them to form a double-stranded RNA stem structure called a panhandle (Elliott, 2014; Malet et al., 2023). This panhandle structure serves as a promoter for transcription and replication

(Malet et al., 2023). Then, nucleoprotein (N) encapsulates each genome segment and associates with the RNA-dependent RNA polymerase (RdRp) to form ribonucleoprotein (RNP) complexes (Sun et al., 2018). These RNP complexes serve as functional templates for synthesizing mRNA and progeny virus genome RNA. Following the completion of this process, the host cell cytoplasm undergoes coordinated replication for all three segments. The RdRp makes complementary positive-sense RNA (cRNA) and progeny negative-sense viral RNA (vRNA) from the RNP complexes (Guu et al., 2011). Then Packaging interactions occur during virus assembly, where the three genome segments interact with the viral glycoproteins Gn and Gc at the Golgi membranes. This interaction is crucial for the proper packaging of all three segments into new virions (Simons & Pettersson, 1991).

When two different bunyaviruses co-infect a cell, the genome segments may mismatch during packaging, potentially leading to the generation of reassortant viruses (Barker et al., 2023). This process involves interactions between genome segments from different viral strains. These interactions ensure the coordinated replication, transcription, and packaging of all three genome segments, which is essential for producing functional progeny viruses.

1.2.4 Bunyavirus Reverse Genetic Systems

Reverse genetics is characterized by the generation of viruses entirely from cloned cDNA. Negative-sense RNA viruses, with genomes complementary to mRNA in orientation, require the provision of viral RNA and proteins for replication and translation to initiate the viral replication cycle. Prior to the recovery of fully infectious viral particles, numerous research groups employed T7- and Pol I-driven minigenome rescue techniques to explore different facets of bunyaviral biology.

Dunn et al. (1995) initially established T7-based bunyaviral minigenome rescue systems by creating a reporter system that enabled the examination of viral transcription requirements via the transfection of a plasmid encoding the negative-sense reporter gene CAT, surrounded by the 5′ and 3′ UTRs of Bunyamwera virus, into cells that express bunyaviral proteins. Flick and Pettersson (2001) subsequently expanded upon this research to create a Pol I-based minigenome rescue system like that described by Dunn et al. for the bunyavirus Uukuniemi virus. This study utilized a minigenome test that involved cotransfection with a GFP reporter gene, bordered by 5′ and 3′ UTR sections of the Uukuniemi virus, into cells containing plasmids that express the L, N, or NSs proteins, or superinfection with the virus itself.

The Flick group successfully adapted this technique for other bunyaviruses, including the Hantaan virus (K. Flick et al., 2003) and the Crimean-Congo hemorrhagic fever virus (R. Flick et al. 2003). The T7- and Pol I-based minigenome rescue systems have been employed by various research groups to explore bunyavirus biology, including critical transcriptional start and termination signals in the 3′ and 5′ terminal genomic regions, cis-acting trafficking and localization signals, and the functional trans-roles of specific viral proteins throughout the viral life cycle (Ikegami et al., 2005; Lopez et al., 1995). These noninfectious minigenome methods have demonstrated efficacy in creating quantifiable, high-throughput reporter systems for screening antiviral agents in lower biosafety level settings for typically high-containment bunyaviruses (Ozawa et al., 2011; Bouloy and Flick, 2009).

Reverse genetic systems for fully infectious clones of bunyaviruses predominantly utilize technology analogous to those employed for orthomyxoviruses and arenaviruses. The Bunyamwera virus, a bunyavirus, was the inaugural segmented, negative-stranded RNA virus to be independently rescued from cloned cDNAs by

Bridgen, Elliott, and their associates, followed by Lowen et al. Complete cDNA replicas of the three bunyavirus genomic segments were inserted into transcription plasmids, which were bordered by the T7 promoter and hepatitis delta virus ribozyme sequences (Bridgen & Elliott, 1996). Upon transfection of these plasmids and expression plasmids encoding for the Bunyamwera viral proteins and the T7 polymerase into mammalian cells, infectious progeny viruses were rescued (Bridgen & Elliott, 1996). The identical T7-based approach was subsequently employed to effectively recover RVFV and La Crosse virus (Bird et al., 2008; Blakqori and Weber 2005). Moreover, additional investigation into viral rescue methodologies by Billecocq et al. (164) and Habjan et al. (2008) demonstrated that a Pol I-based rescue system, involving the cotransfection of Pol I-driven plasmids encoding the L, M, and S genes alongside L and N expression plasmids, constituted a comparably effective approach for rescuing RVFV. Collectively, these investigations have established various reverse genetic techniques for bunyaviruses and expanded the potential applications of recombinant viruses.

1.3 Tofla virus

Tofla virus (TFLV) is a newly identified tick-borne virus that belongs to the genus *Orthonairovirus* in the family *Nairoviridae*. TFLV is classified as a strain of Hazara orthonairovirus and belongs to the Crimean-Congo hemorrhagic fever (CCHF) serogroup. Phylogenetic analyses and neutralization tests have shown that TFLV is closely related to the Hazara virus, which is also part of the CCHF group. Crimean-Congo hemorrhagic fever virus (CCHFV) is known for causing severe hemorrhagic fevers in humans with high mortality rates. TFLV serves as a useful model for studying nairoviruses due to its genetic similarities with other significant viruses in this group.

Understanding its biology and pathogenic potential could help develop preventive measures against tick-borne diseases caused by nairoviruses.

1.3.1 Discovery, prevalence, and disease

Tofla orthonairovirus (TFLV) is a recently identified virus isolated from ticks in Japan. TFLV was discovered in 2013-2014 from ticks collected in Tokushima and Nagasaki prefectures of Japan. It has been detected in two different tick species, *Haemaphysalis flava* and *Haemaphysalis formosensis* species. The virus belongs to the Crimean-Congo hemorrhagic fever (CCHF) group and shares a close relationship with the Hazara virus (Shimada et al., 2016).

TFLV has been identified in ticks collected from different regions in Japan, including Tokushima and Nagasaki, suggesting a potential widespread distribution throughout the country. These tick species are known to feed on wild animals such as deer and wild boars, as well as humans, indicating a possible natural circulation of the virus among these hosts. Although human infections have not been reported, the presence of the virus in ticks that feed on humans raises concerns about potential zoonotic transmission.

In laboratory settings, TFLV virus has shown the ability to cause lethal infections in interferon receptor knockout (IFNAR KO) mice, which are used as models for studying viral pathogenesis1. The infected mice exhibited gastrointestinal disorders, and imaging studies indicated significant uptake of fluorodeoxyglucose in the intestinal tract. The virus can infect and propagate in various cultured cell lines derived from both monkeys and humans (Shimada et al., 2016).

Despite no human cases having been definitively linked to TFLV, the wetland virus (WELV), which was first identified in 2019 in northeastern China, is closely related

to TFLV. WELV can infect humans, causing symptoms such as fever, headache, dizziness, malaise, and arthritis. In some cases, it may lead to neurological complications (Zhang et al., 2024).

While TFLV shows potential pathogenicity similar to other severe Nairoviruses like CCHFV in experimental models, its impact on human health remains uncertain due to the lack of documented human cases. Further research is needed to fully understand its pathogenic potential and epidemiology.

1.3.2 Molecular biology of TFLV

Tofla virus (TFLV) is a member of the genus Orthonairovirus within the family Nairoviridae. Like other orthonairoviruses, it possesses a tripartite negative-sense RNA genome, which is characteristic of this genus. The genome consists of three segments: Large (L), Medium (M), and Small (S) (Fig. 1.1). These segments are linear but form circular structures through non-covalent binding at their terminal sequences. Each segment contains non-coding regions at both 5' and 3' ends. The L segment encodes the RNA-dependent RNA polymerase (RdRp), which plays a crucial role in viral replication and transcription. This segment is 12,143 nucleotides long. The M segment encodes the glycoproteins Gn and Gc, which are crucial for the virus's entry into host cells. This segment is 4,625 nucleotides. The S segment encodes the nucleocapsid protein (N), which encapsulates the RNA segments. It is 1,699 nucleotides long. The genome segments are negative-sense, single-stranded RNA.

The genomic structure of TFLV is closely related to other viruses in the Crimean-Congo hemorrhagic fever group, particularly the Hazara virus. This genomic organization allows TFLV to replicate efficiently in various cell types, including those of human origin, suggesting potential zoonotic capabilities.

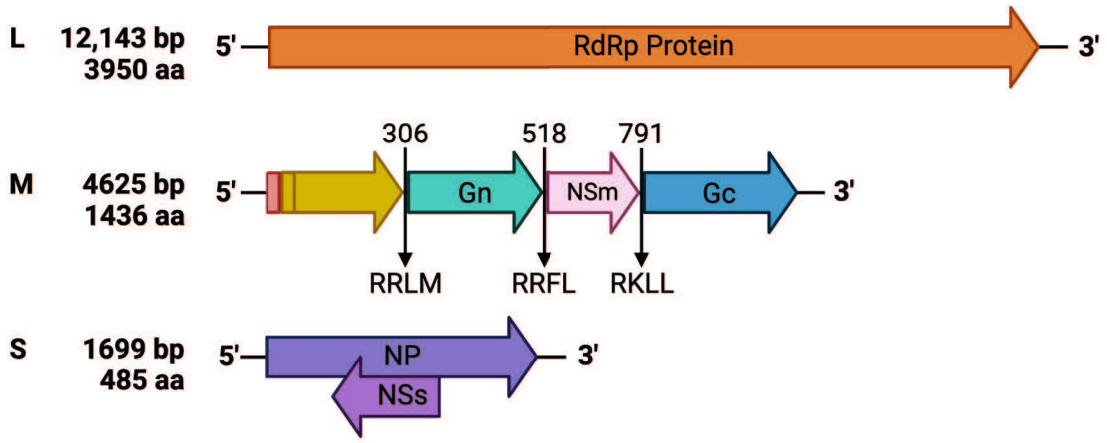

Fig. 1.1 Schematic diagram of the TFLV genome organization. The three genomic segments of TFLV are the large (L), medium (M), and small (S) segments. The S segment encodes the viral nucleoprotein (NP) in one reading frame and the small nonstructural protein (NSs) in an opposite-sense open reading frame. The M segment encodes a glycoprotein precursor (GPC) that is processed by host proteases to produce a mucin-like O-glycosylated region, the Gn and Gc glycoproteins, and the medium non-structural protein (NSm). The L segment of TFLV-encoded protein contains the viral RNA-dependent RNA polymerase (RdRp).

1.4 Severe fever with thrombocytophenia syndrome virus

Severe fever with thrombocytopenia syndrome (SFTS) is an emerging tick-borne zoonotic disease caused by the SFTS virus (SFTSV) and has been a concern since 2009, with an increasing incidence, expanding geographical distribution, and high pathogenicity in East Asia. Cases were reported in China, Japan, South Korea, Vietnam, Taiwan, and Thailand. Infection from SFTSV results in fever, fatigue, gastrointestinal symptoms, thrombocytopenia, and leucopenia in humans, and in some cases, symptoms can progress to severe outcomes, including hemorrhagic disease, multi-organ failure, and even death. Currently, no vaccines or antiviral drugs are available for treatment of the

SFTSV disease. Moreover, little is known about SFTSV-host interactions, viral replication mechanisms, pathogenesis, and virulence, further hampering the development of vaccines and antiviral interventions.

1.4.1 Discovery, prevalence, and disesase

Severe fever with thrombocytopenia syndrome virus (SFTSV) is a novel tick-borne pathogenic bunyavirus and was first identified in 2009 in central China (Yu et al., 2011). SFTSV has since spread to several East Asian countries, raising concerns about its pandemic potential. SFTSV is genetically related to the Heartland virus (HRTV), another highly pathogenic bunyavirus emerging in the United States (Feng et al., 2024). According to the latest International Committee on Taxonomy of Viruses (ICTV) report, SFTSV is classified into the *Bandavirus* genus (*Phenuiviridae* family, *Hareavirales* order) (Genus: Bandavirus | ICTV).

Due to expanding geographical distribution, increasing infection cases, and the potential high pathogenicity, bandaviruses have posed threats to public health and raised more concerns. SFTS prevalence has been increasing in East Asia. China had 18,902 confirmed cases from 2011–2021. Japan as of 2024, nearly 1,000 confirmed cases have been reported, with approximately 100 fatalities. South Korea has reported cases since 2013, primarily in its northern regions (Casel et al., 2021). Taiwan reported its first human case in November 2019 (Lin et al., 2020). Thailand's first case was reported in 2019 (Sansilapin et al., 2024). The disease is primarily found in central, eastern, and northeastern regions of China; western and southern Japan; and northern parts of South Korea.

The case fatality rate varies by country, ranging from 6.18% in China to 27% in Japan and 23.3% in South Korea. Overall, the fatality rate is estimated at 5-15% (Casel

et al., 2021). SFTSV has shown genetic diversity and reassortment. South Korea has identified at least nine distinct genotypes of reassortants (Yun et al., 2019). Seven SFTSV reassortants have been reported in China (Fu et al., 2016). This genetic variability suggests active evolution of the virus in nature, which may impact its spread and virulence.However, to date, there are no specific antiviral drugs and vaccines to control the infections of SFTSV and SFTSV-related viruses.

1.4.2 Molecular biology of SFTSV

Like other members of the *Phenuiviridae* family, the SFTSV genome consists of three single-stranded negative-sense RNA segments defined as large (L), medium (M), and small (S). The L segment encodes RNA-dependent RNA polymerase (RdRp), the M segment encodes a polyprotein precursor that is subsequently cleaved into two glycoprotein subunits, Gn and Gc, and the S segment employs an ambisense coding strategy to encode the nucleoprotein (NP) and the non-structural protein (NSs). The NSs proteins of various pathogenic bunyaviruses, including SFTSV, are considered crucial virulence factors that likely contribute to pathogenesis. The nucleoprotein (NP) encapsulates viral genomic RNA and interacts with RNA-dependent RNA polymerase (RdRp) to generate ribonucleoprotein complexes (RNPs), which are essential constituents of the virion. A diagram of the virion and genomic regions is presented in the figure 1.2.

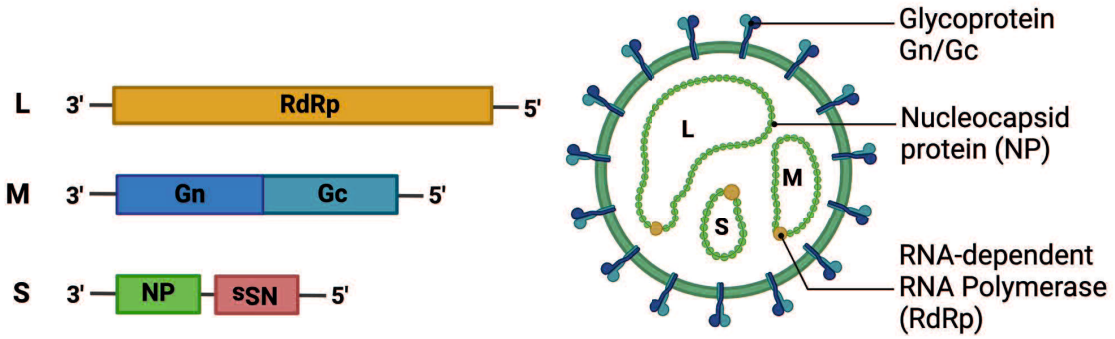

Fig. 1.2 Schematic diagram of the SFTSV virion and genome organization. SFTSV particles are enveloped with the Gn/Gc heterodimers incorporated on the surface. Nucleocapsid protein (NP) and viral RNA-dependent RNA polymerase (RdRp) package the tripartite single-stranded RNA genome (L, M, and S segments) into ribonucleoproteins (RNPs). The L segment encodes RdRp. The M segment encodes Gn and Gc. The S segment encodes NP and nonstructural proteins (NSs) in ambisense orientation.

Chapter 1

Development of an entirely cloned cDNA-based reverse genetics system for Tofla virus of orthonairovirus

2.1 Abstract

The genus Orthonairovirus includes highly pathogenic tick-borne viruses such as the Crimean-Congo hemorrhagic fever orthonairovirus (CCHFV). A reverse genetics system is an indispensable tool for determining the viral factors related to pathogenicity. Tofla orthonairovirus (TFLV) is a recently identified virus isolated from ticks in Japan and our research has suggested that TFLV is a useful model for studying pathogenic orthonairoviruses. In this study, we successfully established a reverse genetics system for TFLV using T7 RNA polymerase. Recombinant TFLV was generated by transfecting cloned complementary DNAs encoding the TFLV genome into BSR T7/5 cells expressing T7 RNA polymerase. We were able to rescue infectious recombinant TFLV mutant (rTFLVmt) and wild-type TFLV (rTFLVpt) viruses, which exhibited indistinguishable growth kinetics in mammalian cells and pathogenicity in A129 mice compared with the authentic virus. Our approach provides a valuable method for establishing reverse genetics system for orthonairoviruses.

2.2 Introduction

The genus Orthonairovirus is classified within the family *Nairoviridae* and the order *Bunyavirales.* This genus includes several pathogenic tick-borne viruses, such as Nairobi sheep disease virus (NSDV) (Orthonairovirus nairobiense), Dugbe virus (Orthonairovirus dugbeense), and Crimean-Congo hemorrhagic fever (CCHF) virus (CCHFV) (Orthonairovirus haemorrhagiae) (Garrison et al., 2020; Burt et al., 1996). These viruses cause severe diseases, including hemorrhagic fever, in both humans and animals (Spengler et al., 2016; Elaldi et al., 2009; Ergo¨nül, 2006; Kar et al., 2020). CCHF is a highly pathogenic illness in humans with a wide geographical distribution owing to the expanding range of tick vectors (Messina et al., 2015; Gargili et al., 2017). NSD causes severe diseases, including hemorrhagic fever, with high mortality in sheep and goats (Davies, 1997). Currently, no effective antiviral agents are available against these viruses. To develop specific treatments for these diseases, it is crucial to elucidate the determinants affecting the pathogenicity of orthonairoviruses.

To identify viral factors related to pathogenicity, *in vitro* and *in vivo* approaches using live viruses based on reverse genetic system are necessary. However, research on live CCHFV is limited because most countries require BSL-4 facilities (maximum containment measures). Alternatively, Hazara virus (HAZV) (Orthonairovirus hazaraense) has been used as a surrogate for CCHFV since it can be used in BSL-2 facilities (Fuller et al., 2019). HAZV was first discovered in *Ixodes redikorzevi* in Pakistan in 1954 (Begum et al., 1970). HAZV shows cross-reactivity with CCHFV, suggesting that it belongs to the CCHFV serogroup (Kal- kan-Yazıcı et al., 2021). Although there is no evidence that HAZV causes infectious diseases in humans and animals, it is pathogenic in experimental mice, such as interferon receptor knockout (IFNAR KO) mice (Dowall et al., 2012).

Tofla virus (TFLV) (Orthonairovirus japonicum) was isolated from ticks in Japan and is closely related to HAZV within the CCHFV group (Shimada et al., 2016). TFLV can infect mammalian cell lines, including human-derived cells, and is lethal in IFNAR-KO mice (Shimada et al., 2016). TFLV has been detected in ticks from various regions of Japan, and multiple strains isolated. Interestingly, we found seropositive wild boars in Nagasaki, Japan, suggesting that TFLV infects wild animals and may cause infectious diseases in mammals (Luvai et al., 2022). Therefore, it is important to elucidate the infectivity and pathogenicity of TFLV in emerging infectious diseases. Additionally, we propose that TFLV could serve as a useful model for studying CCHFV.

The orthonairovirus genome consists of three RNA segments, and the nucleocapsid (N) protein is encoded by the small (S) segment, the glycoprotein precursor GPC (Gn and Gc) by the medium (M) segment, and RNA-dependent RNA polymerase (RdRp) by the large (L) segment (Elliott, 1990). These proteins are essential for the viral replication and transcription of orthonairovirus. The most abundant structural protein is N, responsible for encapsidating the viral genomic segments, while the least abundant protein is RdRp, crucial for viral genome replication and transcription (Carter et al., 2012; Guo et al., 2012; Jeeva et al., 2017; Scholte et al., 2017). Envelope glycoproteins (Gn and Gc) are generated by proteolytic processing from GPC (Sanchez et al., 2002, 2006; Freitas et al., 2020; Hulswit et al., 2021). The TFLV genomic RNA segments and deduced proteolytic sites in the Gn and Gc were similar to those of other orthonairoviruses (Shimada et al., 2016).

Reverse genetic systems have been established to enable researchers to manipulate viral genomes, study their functions, and investigate their interactions with host cells. This technology has also been applied to orthonairoviruses (Fuller et al., 2019; Flick et al., 2003). The generation of artificial viral RNA genome segments using the

RNA polymerase I system was developed for CCHFV, facilitating the study of viral biology and the development of antiviral drugs (Flick et al., 2003). HAZV has a reverse genetics system that allows the rescue of infectious cDNAs. These systems have been used to examine the role of caspase cleavage sites within the HAZV nucleocapsid protein, demonstrating that this sequence plays a critical role in the viral life cycle (Fuller et al., 2019).

In this study, we aimed to develop a reverse genetics system for TFLV using cloned cDNA and a T7 polymerase plasmid. This system involves cloning the cDNAs encoding the three antigenomic segments into transcription vectors controlled by the T7 promoter and hepatitis delta virus ribozyme sequences. Transfection of these vectors, along with helper plasmids expressing the nucleoprotein and viral RNA-dependent RNA polymerase, into BSR T7/5 cells constitutively expressing T7 pol, efficiently rescued the recombinant TFLV.

2.3 Materials and methods

2.3.1 Virus and cells

The stock virus of the TFLV Tok-Hfla-2013 strain (Shimada et al., 2016) was prepared from Vero E6 (African green monkey kidney) cell culture medium. A549 (human), Fcwf-4 (cat), DM-WFLT (wild boar), Vero E6, and BSR-T7/5 cells were grown in Dulbecco's modified Eagle's minimum essential medium (DMEM) (Gibco; Thermo Fisher Scientific, MA, USA) supplemented with 10% heat-inactivated fetal bovine serum (FCS) (Serana Europe GmbH, Pessin, Germany), and 1% penicillin-streptomycin (100 U/ml penicillin, and 100 μg/ml streptomycin; FUJIFILM, Wako Pure Chemical Corporation, Osaka, Japan). Cells were incubated in a CO2 incubator at 37 °C. BSR-T7/5 cells derived from baby hamster kidney (BHK) cells stably expressing T7 RNA polymerase were kindly provided by Dr. K. K. Conzelmann (Max-von-Pettenkofer Institute, Munich, Germany) (Buchholz et al., 1999). The infectious titers of the TFLV stocks were assessed using a focus-forming assay (FFA). All experiments with infectious viruses were conducted in a biosafety level 3 (BSL-3) facility at Yamaguchi University according to the standard BSL-3 guidelines.

2.3.2 FFA of TFLV

The FFA of TFLV was performed as described previously (Shimada et al., 2016). Briefly, confluent Vero E6 cells were infected with serial dilutions TFLV and incubated in overlay DMEM containing 2% FCS and 1% methylcellulose 4,000 (Wako Pure Chemical Industries, Ltd., Tokyo, Japan) in CO2 incubator at 37°C. After three days, the cells were washed with PBS and fixed with 4% formaldehyde. The fixed cells were incubated with a 1:500 dilution of TFLV antiserum for 1 h. This was followed by incubation with a 1:1000 dilution of peroxidase-conjugated anti-mouse IgG antibody

(American Qualex). Viral foci were visualized using DAB substrate (Wako Pure Chemical Industries Ltd., Tokyo, Japan). Viral titers are indicated as focus-forming units per ml (FFU/ml).

2.3.3 Total cell RNA Extraction and One Step RT-PCR

Total cellular RNA was extracted from the supernatant of TFLV-infected Vero E6 cells by using ISOGEN-LS (Nippon Gene) or from the cells using ISOGEN-II (Nippon Gene). cDNA fragments were amplified with specific primers (Table 2.1) using OneStep RT-PCR (QIAGEN). This included one fragment of the S segment (S), two fragments of M segment (M1 and M2), and three fragments of the L segments (L1, L2, and L3). The PCR products were excised from the gel and purified using a MinElute Gel Extraction Kit (QIAGEN), followed by direct nucleotide sequencing of the PCR product.

Table 2.1 Oligonucleotides utilized for amplification of TFLV fragments

Primer	Fragment	Sequence (5'-3')	Nucleotide Position
S Segment			
TFLV-S1F	S	TCTCAAAGACAAACGTGCCG	1-20
TFLV-S1699R	S	TCTCAAAGATATCGTTGCCG	1679-1699
M Segment			
TFLV-M1F	M1	TCTCAAAGACAGACTTGCGG	1-20
TFLV-M1921R	M1	CAGGTGCCAGAGTCACTAGG	1920-1940
TFLV-M1861F	M2	CTTGAATTTCGGCATCCTAC	1841-1861
TFLV-M4625R	M2	TCTCAAAGACAGACTTGCGG	4605-4625
L Segment			
TFLV-L1F	L1	TCTCAAAGACATCAATCCCCCA	1-22
TFLV-L3121R	L1	GCATCTGGTGCCCTGAAGGT	3120-3140
TFLV-L3061F	L2	ATGAGCTCAATGTTAACCGC	3041-3061
TFLV-L8521R	L2	TAGGACATTCAATATGCACT	8520-8540
TFLV-L8451F	L3	CTAGTCGACTCGTGCGCATG	8431-8451
TFLV-L12143R	L3	TCTCAAAGATATCGTTGCCC	12123-12143

2.3.4 Subcloning of full-length sequences of TFLV S, M, and L segments

Each fragment was subcloned into the pCR II-TOPO vector (Invitrogen) as TOPO-TFLV-S, TOPO-TFLV-M1, TOPO-TFLV-M2, TOPO-TFLV-L1, TOPO-TFLV-L2, and TOPO-TFLV-L3. TOPO-TFLV-M1 and TOPO-TFLV-M2 were digested with *BlpI* and *NotI* and ligated to generate the full-length sequence of the M segment (TOPO-TFLV-M). TOPO-TFLV-L1, TOPO-TFLV-L2, and TOPO-TFLV-L3 were digested with *NotI, HpaI,* and *NruI* and ligated to generate the full-length sequence of the L segment (TOPO-TFLV-L).

2.3.5 Construction of plasmids providing TFLV genomic RNA

Plasmid for the recovery of TFLV was created based on previously described systems for Rift Valley fever virus and Severe fever and thrombocytopenia syndrome virus (SFTSV) (Brennan et al., 2015; Billecocq et al., 2008). Viral RNA transcription plasmids were constructed by inserting the full-length S, M, and L of TFLV into the TVT7R vector, kindly provided by Dr. Benjamin Brennan (Glasgow Centre for Virus Research, Scotland, United Kingdom) (Brennan et al., 2015). TOPO-TFLV-S, TOPO-TFLV-M, and TOPO-TFLV-L were used as template cDNAs. Full-length S, M, and L segments of TFLV were amplified with segment-specific oligonucleotide (Table 2.1) using CloneAmp HiFi PCR Premix (Takara). The TVT7R vector, linearized by PCR with primer pairs, shared a homologous sequence with each end of the TFLV segment. The TVT7R vector was linearized for the TFLV S, M, and L segments using the following primers: TFLV_S_VF and TFLV_S_VR, TFLV_M_VF and TFLV_M_VR, and TFLV_L_VF and TFLV_L_VR (Table 2.2). Viral anti-genomic cDNAs was cloned into the TVT7R linearized vector using In-Fusion HD restriction-free cloning (Clontech). The resultant plasmids were pTVT7-TFLV-S, pTVT7-TFLV-M, and pTVT7-TFLV-L,

which contained full-length cDNAs in an antisense orientation flanked by the T7 promoter and the hepatitis delta ribozyme sequence (Fig 2.1.A).

Table 2.2 Oligonucleotides utilized for the pTVT7 S, M, and L TFLV plasmid construction

Primer for Linearized Vector	Sequence (5'-3')[a]
pTVT7 S	
TFLV_S_VF	caacgatatctttgaga*GGGTCGGCATGGCATCTCC*
TFLV_S_VR	cgtttgtctttgagaCTATAGTGAGTCGTATTAATTTC
pTVT7 M	
TFLV_M_VF	cacgatatctttgaga*GGGTCGGCATGGCATC*
TFLV_M_VR	caagtctgtctttgagaCTATAGTGAGTCGTATTAA
pTVT7 L	
TFLV_L_VF	caacgatatctttgagaGGGTCGGCATGGCATCTC
TFLV_L_VR	gattgatgtctttgagaCTATAGTGAGTCGTATTAA

[a]Uppercase, vector-derived sequences; lowercase, viral sequences; italics, hepatitis delta ribozyme sequence; and underlined, T7 promoter sequence.

2.3.6 Construction of helper plasmids providing nucleocapsid and RdRp of TFLV

Helper plasmids for the expression of TFLV nucleoproteins and viral RdRp were constructed by inserting open reading frames (ORFs) into the linearized pTM1 vector using In-Fusion HD restriction-free cloning (Clontech). The pTM1 vector was linearized by PCR using primers TFLV_pTM1S_VF and TFLV_pTM1S_VR for pTM1-N and TFLV_pTM1L_VF and TFLV_pTM1L_VR for pTM1-L (Table 2.3). The ORFs of TFLV N and RdRp were amplified using the primers TFLV_pTM1S_IF and TFLV_pTM1S_IR and TFLV_pTM1L_IF and TFLV_pTM1L_IR, respectively (Table 3). The constructed plasmids were designated pTM1-TFLV N and pTM1-TFLV L, and were placed under the control of the T7 promoter and encephalomyocarditis virus internal ribosome entry site sequences (Fig 2.1.A).

Table 2.3 Oligonucleotides utilized for the pTM1 S and L TFLV plasmid construction

Primer	Amplification	Sequence (5'-3')[a]
pTM1 S		
TFLV_pTM1S_VF	Vector	caacatcaacatcatctaa*CTCGAGAGGCCTAATTAA*
TFLV_pTM1S_VR	Vector	acaatcttgttctccat**GGTATTATCGTGTTTTTCAAAG**
TFLV_pTM1S_IF	Insert	atggagaacaagattgtcgcagagtccc
TFLV_pTM1S_IR	Insert	ttagatgatgttgatgttggttgcattgccc
pTM1 L		
TFLV_pTM1L_VF	Vector	tcaattgggacagtgactga*CTCGAGAGGCCTAATTAATTAAG*
TFLV_pTM1L_VR	Vector	gccctcaaggaaatccat**GGTATTATCGTGTTTTTCAAAG**
TFLV_pTM1L_IF	Insert	atggatttccttgagggcatcgtgtgg
TFLV_pTM1L_IR	Insert	tcagtcactgtcccaattgaatgtgaagcctct

[a]Uppercase, vector-derived sequences; lowercase, viral sequences; italics and underlined, 3' cloning site of pTM1; bold, 5' cloning site of pTM1

2.3.7 Infectious virus rescue by the Reverse Genetics System

Approximately 80% confluent BSR T7/5 cells were seeded in plastic dishes. A mixture of plasmids comprising 2 μg each of pTVT7-TFLV-S, pTVT7-TFLV-M, pTVT7-TFLV-L, pTM1-TFLV-S and 0.2 μg of pTM1-TFLV-L in Opti-MEM Medium (Thermo Fisher Scientific) were transfected into the BSR T7/5 cells using TransIT-LT1 reagent (Mirus Bio LLC, Madison, WI, USA) (Fig 2.1.B). Transfected cells were incubated for 5 days at 37 °C, and the supernatant was inoculated in Vero E6 cells prepared in a flask, and the supernatant was harvested after 5 days. The infection-rescued viruses were confirmed using FFA. The genome sequences of the recovered viruses were determined by Sanger sequencing.

2.3.8 Viral growth kinetics of TFLV in cultured cell lines

The growth kinetics of the authentic and recombinant viruses were compared in Vero E6, A549, Fcwf-4, and DM-WFLT cells at a multiplicity of infection (MOI) of 0.001 in 12 well-plates. Supernatant samples were collected at 0, 24, 48, 72, 96, and 120 h post infection (hpi). The supernatants were centrifuged at 3,500 rpm for 5 minutes to remove debris and stored at −80 °C. The viral titers of the supernatant samples were determined using FFA.

2.3.9 Infections of TFLV in mice

A129 mice were purchased from B&K Universal Limited and mated at Yamaguchi University, Japan. Six to eight-week-old mice were subcutaneously infected with 1 FFU of TFLV (n = 5). The mice were monitored daily for clinical signs of disease, body weight, and survival. Animal experiments were performed in accordance with the recommendations of the Fundamental Guidelines for the Proper Conduct of Animal Experiments and Related Activities in Academic Research Institutions under the jurisdiction of the Ministry of Education, Culture, Sports, Science, and Technology. The Animal Care and Use Committee of Yamaguchi University approved all experimental protocols (approval number: 05-31-565).

2.4 Results

2.4.1 Construction of plasmids for the reverse genetics system of TFLV

The T7-driven plasmids pTVT7 and pTM1 were used for the reverse genetics of TFLV based on a previous study (Brennan et al., 2015). First, the full-length genome sequences of the S, M, and L segments were subcloned into the pCR II-TOPO vector. The pTVT7 plasmid was designed to contain each full-length genome segment flanked by the T7 promoter and hepatitis delta virus (HDV) ribozyme sequences. Plasmids pTVT7-TFLV-S, pTVT7-TFLV-M, and pTVT7-TFLV-L were generated to transcribe the S, M, and L segments, respectively (Fig. 2.1.A). Plasmids pTM1-TFLV-S and pTM1-TFLV-L were constructed to produce the N protein and RdRp, respectively (Fig. 2.1.A).

First-generation pTVT7-TFLV-S, pTVT7-TFLV-M, and pTVT7-TFLV-L (rTFLVmt) contained eight non-synonymous mutations compared to authentic TFLV, without synonymous substitutions (Table 2.4). Therefore, these mutations were replaced by the original sequences of TFLV (rTFLVpt) to create the corrected plasmids.

Table 2.4 Nucleotide and amino acid mutations in recombinant-rescued TFLV

Segment	Nucleotides	Protein	Parent	rTFLV-wt	rTFLV-mut
S	1212	N	t (Met)	t (Met)	c (Thr)
M	2390	Gc	a (Asp)	a (Asp)	g (Gly)
L	8985	L	g (Asp)	g (Asp)	a (Asn)
	9099	L	t (Ser)	t (Ser)	a (Thr)
	9523	L	a (Tyr)	a (Tyr)	g (Cys)
	10606	L	t (Met)	t(Met)	c (Thr)
	11037	L	a (Thr)	a (Thr)	g (Ala)
	11122	L	a (Lys)	a (Lys)	g (Arg)

2.4.2 Rescue of recombinant TFLV from constructed plasmids

To recover infectious viruses from the cloned cDNA, pTVT7-TFLV-S, pTVT7-TFLV-M, pTVT7-TFLV-L, pTM1-TFLV-S, and pTM1-TFLV-L were simultaneously transfected into BSR T7/5 cells stably expressing T7 RNA polymerase (Fig 2.1.B). At 5 days post-transfection (dpi), the supernatant was harvested and infectious virus production was confirmed by FFA. Focus morphology was similar between rTFLVmt, rTFLVpt, and the parent TFLV (Fig. 2.1.C). Viral titers of the supernatants from rTFLVmt and rTFLVpt viruses were 4.3 x 10^3 FFU/ml and 3.97 x 10^3 FFU/ml, respectively. The sequences of the rescued viruses were identical to those of rTFLVmt and rTFLVpt. The rTFLVmt and rTFLVpt viruses were then inoculated into Vero E6 cells and prepared as stock viruses for further experiments. A single passage into Vero E6 cells increased the titer of the rescued viruses. Viral titers of the stocked viruses rTFLVmt and rTFLVpt were 3.8 x 10^4 ffu/ml and 3.39 x 10^4 ffu/ml, respectively. Based on these results, we successfully established a reverse genetics system for TFLV.

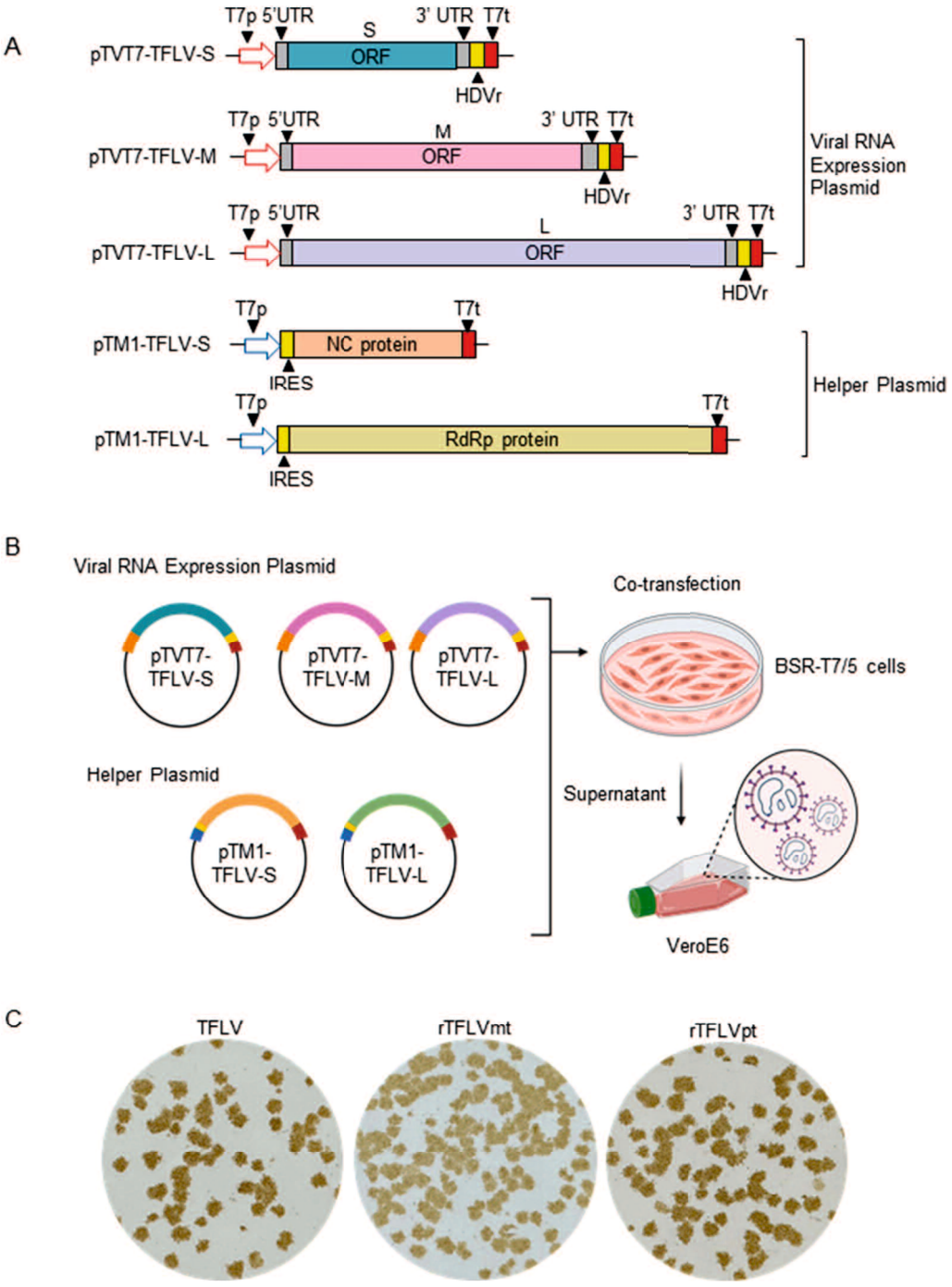

Fig. 2.1 Schematic representation of a plasmid-based reverse genetics system to rescue infectious TFLVs from cloned cDNAs. (A) Generating viral RNA expression plasmids contain full-length cDNAs in antigene sense orientation flanked by the T7 promoter (T7p) and hepatitis delta virus ribozyme (HDVr). Helper plasmids contain the N and RdRp ORFs under the control of the T7 promoter (T7p), T7 terminator (T7t), and the encephalomyocarditis virus internal ribosome entry site sequence (IRES). (B) Transfection strategy to rescue the recombinant TFLVs. BSR-T7/5 cells were co-transfected with T7 RNA polymerase-driven plasmids to generate S, M, and L viral genomes and helper plasmids to supply viral N and RdRp proteins to the cells. The resulting recombinant virus in BSR-T7/5 was passed into Vero E6 cells. (C) Comparisons of foci appear from the focus-forming assay of parent TFLV, recombinant TFLV mutant (rTFLVmt), and wild-type TFLV (rTFLVpt) viruses.

2.4.3 Infectivity of rescued viruses in cultured cell lines derived from mammals

The infectivity and growth kinetics of rTFLVmt and rTFLVpt were compared with those of authentic TFLV. Vero E6 (African green monkey), A549 (human), Fcwf-4 (cat), and DM-WFLT (wild boar) cells were inoculated with rTFLVmt, rTFLVpt, and parent TFLV, and the viral titers of the supernatants at 0–120 hpi were compared. rTFLVmt, rTFLVpt, and parent TFLV showed similar growth curves in all cell lines (Fig. 2.2.A). Viral titers peaked at 3 days post-infection (dpi) in Vero E6, A549, and Fcwf-4 cells and at 1 dpi in DM-WFLT cells (Fig 2.2.A). These observations indicate that rescued rTFLVmt and rTFLVpt showed similar infectivity and growth kinetics to the parent TFLV in mammalian-derived cell lines.

Notably, Fcwf-4 cells showed a prominent cytopathic effect (CPE) at 5 dpi, whereas Vero E6, A549, and DM-WFLT cells did not (Fig. 2.2.B). CPE was observed in infections with rTFLVmt, rTFLVpt, or parent TFLV.

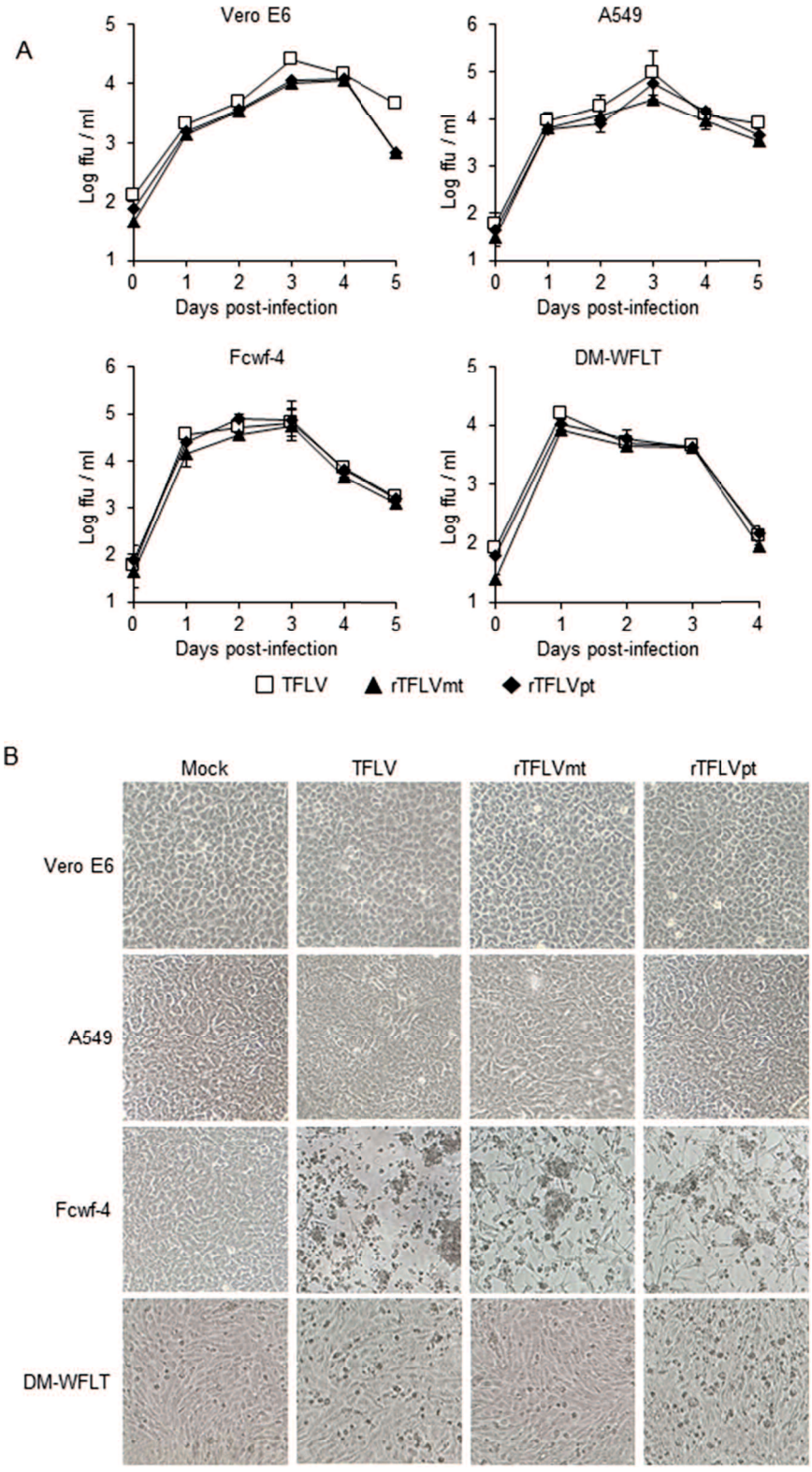

Fig. 2.2 Susceptibility of TFLVs in different cell lines. (A) Growth kinetics of infectious viral titers in the supernatants of Vero E6, A549, Fcwf-4, and DM-WFLT infected with parental TFLV, rescued rTFLVmt, and rTFLVpt at MOI of 0.001 (N = 3). Viral titers were determined by the FFA. Error bars indicate standard errors. (B) Morphological changes of cell cultures infected with parental TFLV, rescued rTFLVmt and rTFLVpt at 5 dpi in Vero E6, A549, Fcwf-4, and DM-WFLT. Cells were infected at MOI of 0.001. Significant CPEs were observed in Fcwf-4 cells.

2.4.4 Virulence of rescued viruses in A129 mice

The pathogenicity of the rescued viruses *in vivo* was compared to that of the parent TFLV. A129 mice were infected with rTFLVmt, rsTFLV, or parent TFLV, and their daily clinical signs and survival were observed. All mice infected with each virus died at 3–5 dpi, and there were no significant differences in the survival curves between the rTFLVmt, rsTFLV, and parent TFLV groups (Fig. 2.3). These results indicate that the rescued viruses rTFLVmt and rTFLVpt showed similar pathogenicity in A129 mice as the original TFLV.

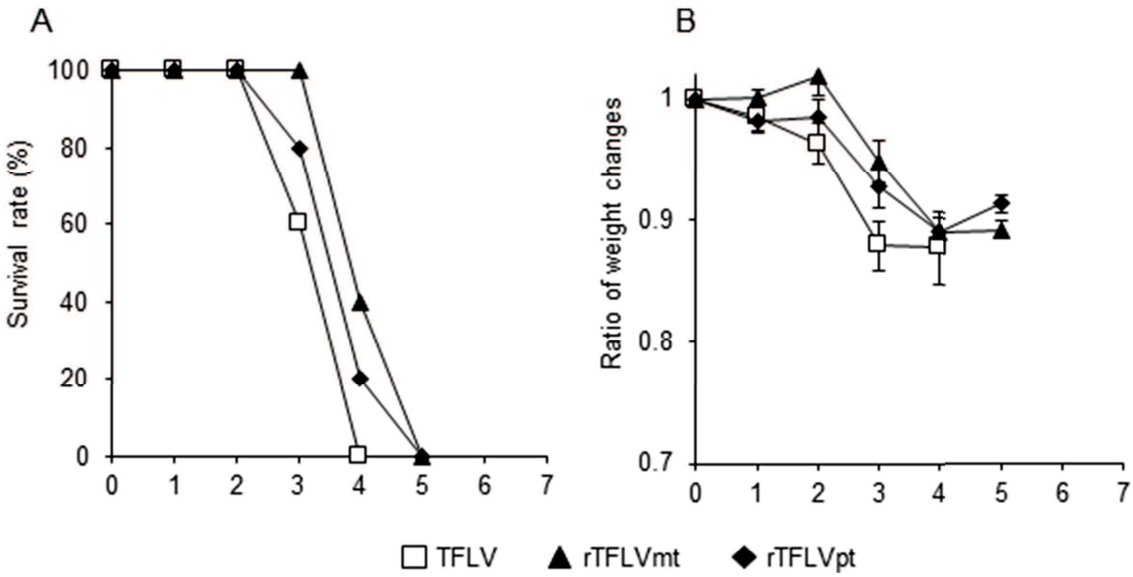

Fig. 2.3 Pathogenicity of TFLVs in A129 mice. (A) Survival curves and (B) Body weight changes of A129 mice (n = 5) subcutaneously inoculated with 1 ffu of parental TFLV, rescued rTFLVmt, and rTFLVpt. Relative body weight is shown as means with standard errors.

2.5 Discussion

In this study, we established a reverse genetics system for TFLV, belonging to the genus *Orthonairovirus*. Reverse genetics is an essential method for analyzing the role of viral genes; however, the complexity and large size of the L segment in this group, compared to other bunyaviruses, could potentially reduce the efficiency of reconstituting RNPs. Therefore, establishing an efficient reverse genetics system remains a challenge. The reverse genetics of these two orthonairoviruses have been reported. First, the RNA polymerase I (polI) system successfully produced a rescue virus for CCHFV (Flick et al., 2003). The development of a minigenome system for the CCHFV rescue system and entirely cloned cDNA transfection have also been reported (Scholte et al., 2017; Bergeron et al., 2010, 2015). Second, the recovery of HAZV from cDNA using the minigenome system has also been reported (Fuller et al., 2019; Matsumoto et al., 2019). In this study, we used T7 RNA polymerase-driven reverse genetics systems in BSR-T7/5 cells stably expressing T7 RNA polymerase for SFTSV (Brennan et al., 2015). Our preliminary experiments indicated that viral growth of TFLV was not high in BSR-T7/5 cells, suggesting that viral replication of TFLV may not be optimally effective in the cells. Therefore, it was considered that in BSR-T7/5 cells, NC protein and RdRp, which are required for the reconstitution of the SFTSV transcription complex to synthesize viral RNA, were mainly supplied from pTM1-TFLV-S and pTM1-TFLV-L, respectively. Our approach was different from those of CCHFV and HAZV and represents the first reverse genetics system for TFLV. Our study provides a selective method for establishing a reverse genetics system for other orthonairoviruses.

Viral genome cloning is a critical step in the construction of a reverse genetics system for TFLV. However, the plasmid construction of viral genes frequently causes unexpected mutations during plasmid propagation in *Eschericia coli*. In this study, the

first plasmids generated to produce TFLV RNAs (pTVT7-TFLV-S, pTVT7-TFLV-M, and pTVT7-TFLV-L) contained eight nucleic acid mutations with amino acid changes compared to the original TFLV. Using subcloning, we constructed plasmids containing the original TFLV sequences. Notably, the rTFLVmt virus showed similar infectivity and growth curves in cultured cells and pathogenicity in A129 mice compared to the parent TFLV and rTFLVpt viruses, suggesting that mutations seen in rTFLVmt do not influence the properties of TFLV.

We previously showed that TFLV infected human- and monkey-derived cell lines and was lethal in IFNAR-KO mice, leading to gastrointestinal disorders (Shimada et al., 2016). In this study, we showed that TFLV infection propagated in feline and wild boar-derived cell lines. These observations suggest that TFLV can infect various mammalian cells. Interestingly, TFLV infection induced prominent CPE in feline-derived Fcwf-4 cells, but not in Vero E6, A549, or DM-WFLT cells. The CPE of the Fcwf-4 cell was observed at 5 dpi, whereas the peak of viral titer in the supernatant was at 3 dpi. Although the timing and viral titer of the peak in Vero E6 and A549 were similar to those of Fcwf-4 cells, CPEs were not observed at 4 and 5 dpi in those cells. The peak of viral titer in DM-WFLT cells was at 1 dpi, but CPE was not observed at 2 to 4 dpi. In a previous study, human-derived SK-N-SH, T98G, and HEK293 cells did not show CPE after TFLV infection (Shimada et al., 2016). Elucidation of the mechanism of CPE induction in Fcwf-4 cells compared to other cell lines may provide interesting insights into the pathogenicity of TFLV in mammalian cells.

We have previously shown that there are seropositive wild boars in Nagasaki, Japan, suggesting that TFLV infects wild animals and may cause infectious diseases in mammals (Luvai et al., 2022). Recently, several orthonairoviruses were identified in ticks in Japan (Oba et al., 2015; Kodama et al., 2021). Of note, Yezo virus (YEZV) was

isolated from human cases with acute febrile illness in Hokkaido, Japan (Kodama et al., 2021). Therefore, there is a possibility that TFLV also causes emerging infectious diseases in humans and animals. Investigation of pathogenicity, preparation of diagnostic methods, and epidemiological surveys are important priorities for preemptive countermeasures against this new tick-borne orthonairovirus.

The TFLV reverse genetics system will facilitate further studies to fully understand the potential impact of TFLV on human and animal health as well as the biology of othonairoviruses in general. In addition, we raise the possibility that TFLV is a useful CCHFV model.

2.6 Conclusion

The reverse genetics of orthonairoviruses has remained challenging compared to that of other bunyaviruses due to the complexity and large size of the L segment, which could potentially reduce the efficiency of reconstituting RNPs. In this study, we established a TFLV system using a T7 RNA polymerase-driven approach. This provides an alternative method for orthonairovirus systems.

We have previously shown that there are seropositive wild boars, suggesting that TFLV infects wild animals and may cause infectious diseases in mammals. Therefore, reverse genetics is a useful tool for investigating viral genes responsible for pathogenicity, serving as a preemptive countermeasure against this new tick-borne orthonairovirus.

TFLV is closely associated with HAZV in the CCHFV group. TFLV can infect mammalian cell lines, including human-derived cells, and is lethal in IFNAR-KO mice. Therefore, we propose that TFLV is a potential surrogate and model system for research on CCHFV.

Chapter 2

Two amino acid pairs in the Gc glycoprotein of severe fever with thrombocytopenia syndrome virus responsible for the enhanced virulence

3.1 Abstract

Severe fever with thrombocytopenia syndrome (SFTS) is a significant public health concern, with a high fatality rate in humans and cats. In this study, we explored the genetic determinants that contribute to the different virulence of SFTS virus (SFTSV) based on Tk-F123 and Ng-F264 strains isolated from cats. Tk-F123 was 100% lethal in type I interferon receptor knockout mice, whereas Ng-F264 exhibited no fatality. We identified a pair of amino acid residues in the Gc protein, glycine and serine, at residues 581 and 934, respectively, derived from Tk-F123, leading to a fatal infection. Those in Ng-F264 were arginine and asparagine. These results suggest that this pair of residues affects the Gc protein function and regulates SFTSV virulence. Our findings provide useful clues for the elucidation of viral pathogenicity and the development of effective live-attenuated vaccines and antiviral strategies.

3.2 Introduction

Severe fever with thrombocytopenia syndrome (SFTS) is an emerging tick-borne viral disease that poses significant public health concerns in most Asian countries (Ando et al., 2021; Yu et al., 2011; Takahashi et al., 2013; Park et al., 2014; Tran et al., 2019). The causative agent of the SFTS virus (SFTSV) (*Bandavirus dabieense*) is classified within the genus Bandavirus of the family Phenuviridae and order Hareavirales (Genus: Bandavirus | ICTV). SFTSV is transmitted to humans and animals through ticks such as *Haemaphysalis longicornis* (Xing et al., 2017).

In humans, SFTS symptoms include fever, enteritis, thrombocytopenia, and leukopenia, with mortality rates of up to 30% (Takahashi et al., 2013). Cats are sensitive to SFTSV infection and show clinical signs similar to those of humans, including gastrointestinal signs, thrombocytopenia, and leukopenia, with a fatality rate as high as 60% (Ando et al., 2021; Osako et al., 2024). Cat-to-human transmission has been reported (Yamanaka et al., 2020), which increases the risk of zoonosis.

The SFTSV genome comprises three RNA segments, negative sense and ambisense, which are referred to as small (S), medium (M), and large (L) (Yu et al., 2011, 2012; Lei et al., 2015). The S segment encodes the viral nucleocapsids and nonstructural proteins (NSs). The M segment encodes the viral glycoproteins (GPs), which are subsequently cleaved into two essential viral envelope glycoproteins, Gn and Gc. The L segment encodes viral RNA-dependent RNA polymerase (RdRp), also known as the L protein (Yu et al., 2011).

The high pathogenicity of SFTS appears to be caused by both viral and host factors. Experimental mouse models have been used to elucidate the disease mechanisms *in vivo*. Type I interferon (IFN-I) receptor (IFNAR)-deficient mice are highly susceptible to SFTSV infection (Liu et al., 2017). This increased susceptibility highlights the critical

role of IFN-I. Absence of this response allows unrestricted viral growth and dissemination, leading to severe clinical outcomes (Park et al., 2020). Previous studies have reported that SFTSV NSs antagonize the IFN-I response and that their interaction with signal transducer and activator of transcription 2 (STAT2) determines the species-specific pathogenicity of SFTSV (Yoshikawa et al., 2023).

To evaluate the viral factors, a reverse genetics system for SFTSV was employed to identify the key genetic determinants that contribute to SFTSV pathogenicity (Brennan et al., 2015). NSs are considered virulence factors of SFTSV because NSs deletions or mutations disturb the innate immune response and reduce virulence in highly susceptible IFNAR-deficient mice (Yu et al., 2019; Bryden et al., 2022; Shimojima et al., 2024). Furthermore, an aged ferret model demonstrated the potential of recombinant NSs viruses as vaccine candidates (Yu et al., 2019). Infection with a mutant SFTSV lacking the N-linked glycosylation motif in glycoproteins reduces virulence in IFNAR-deficient mice (Shimojima et al., 2024). The amino acid mutation E251K on the surface of RdRp has been reported to enhance the viral replication rate and *in vivo* virulence (Jeon et al., 2023). These findings suggest that multiple genetic factors contribute to SFTSV virulence.

In our previous study, we compared the virulence of several SFTSV strains isolated from cats in Nagasaki, Japan, including fatal and recovered cases, in IFNAR-knockout (A129) mice (Ando et al., 2021). This resulted in 0–100% fatality in A129 mice, suggesting that various genes cause high or low pathogenicity in mice among the different strains (Ando et al., 2021). In addition, we are currently investigating the genetic and pathogenic properties of SFTSV based on comparisons with multiple SFTSV strains isolated from animals in various regions of Japan (unpublished data). In these experiments in the present study, we identified virulent and avirulent SFTSV strains in

A129 mice, with 100% and 0% mortality, respectively. In this study, we attempted to determine the viral genes responsible for the virulence in a mouse model using the virulent and avirulent strains based on SFTSV reverse genetics.

3.3 Materials and Methods

3.3.1 Cells and Viruses

BSR-T7/5 cells stably expressing T7 RNA polymerase were kindly provided by Dr. K. K. Conzelmann (Max-von-Pettenkofer Institut, Munich, Germany) (Buchholz et al., 1999) and Vero E6 (African green monkey kidney) were grown in Dulbecco's modified Eagle's minimum essential medium (DMEM) (Gibco; Thermo Fisher Scientific, MA, USA) supplemented with 10% heat-inactivated fetal bovine serum (FBS) (Serana Europe GmbH, Pessin, Germany), 1% penicillin-streptomycin (100 U/ml penicillin, and 100 μg/ml streptomycin; FUJIFILM, Wako Pure Chemical Corporation, Osaka, Japan). Cell lines were cultured at 37°C in a 5% CO_2 incubator. SFTSV strains Tk-F123 and Ng-F264 were isolated from cats in Tokushima and Nagasaki, Japan, respectively. The stock virus of SFTSV was propagated in Vero E6 cells in DMEM containing 2% FBS at 37 °C in a 5% CO_2 incubator, and the culture medium was harvested 5 days post-infection (dpi). The infectious titers of the SFTSV stocks were assessed using a focus-forming assay. All experiments using infectious SFTSV were carried out in a biosafety level 3 (BSL-3) facility at Yamaguchi University according to standard BSL-3 guidelines.

3.3.2 Focus-forming assay

Confluent Vero E6 cells were infected with a serial dilution of SFTSV and incubated in an overlay DMEM containing 2% FCS and 1% methylcellulose 4,000 (Wako Pure Chemical Industries, Ltd., Tokyo, Japan) in a CO_2 incubator at 37°C. At 3 dpi, cell monolayers were fixed with 4% formaldehyde. Following fixation, the cell monolayers were incubated with a 1:500 dilution of SFTSV monoclonal antibody for 1 h. This was followed by incubation with a 1:1000 dilution of peroxidase-conjugated anti-

mouse IgG antibody (American Qualex, CA, USA). Viral foci were visualized using a 3,3'-diaminobenzidine tetrahydrochloride (DAB) substrate (Wako Pure Chemical Industries Ltd., Tokyo, Japan). Viral titers are indicated as focus-forming units (FFU)/ml.

3.3.3 Mouse experiment

The A129 mice were purchased from B&K Universal Limited and mated at Yamaguchi University, Japan. Five-to seven-week-old mice were subcutaneously infected with 10^4 FFU of SFTSV. Mice were monitored daily for clinical signs of disease, body weight, and survival. The animal experiments were performed in accordance with the Fundamental Guidelines for the Proper Conduct of Animal Experiments and Related Activities in Academic Research Institutions under the jurisdiction of the Ministry of Education, Culture, Sports, Science, and Technology. The Animal Care and Use Committee of Yamaguchi University approved all the experimental protocols (approval number: 05-31-565).

3.3.4 RNA Extraction, RT-PCR, and sequencing

Viral RNA was extracted from the culture supernatant using ISOGEN-LS (Nippon Gene Co., Ltd., Toyama, Japan) and from the cells using ISOGEN-II (Nippon Gene Co., Ltd., Toyama, Japan). The extracted RNA was amplified using a One-Step RT-PCR (QIAGEN, Foster City, California, USA) according to the manufacturer's instructions. Final products were purified using the MinElute Gel Extraction Kit (QIAGEN, Hilden, Germany) and sequenced by a commercial service company (Eurofins Genomics, Tokyo, Japan).

3.3.5 Construction of infectious recombinant SFTSV

Recombinant SFTSV was rescued using a reverse genetics system in BSR T7/5 cells based on a previously described system for SFTSV (Brennan et al., 2015). Plasmids were constructed by inserting the full-length S, M, and L from the Tk-F123 and Ng-F264 strains into the TVT7R vector, kindly provided by Dr. Benjamin Brennan of the Glasgow Centre for Virus Research, Scotland, United Kingdom (Brennan et al., 2015). Recombinant viruses from cDNA were generated by transfecting BSR T7/5 cells using a TransIT-LT1 reagent (Mirus Bio LLC, Madison, WI, USA) with a mixture of plasmid sets in 200 μL of Opti-MEM Medium (Thermo Fisher Scientific, Waltham, Massachusetts, USA), according to the manufacturer's protocol. Following viral propagation, rescued viruses were confirmed using a focus-forming assay. The genome segments of the recovered viruses were amplified using OneStep RT-PCR (QIAGEN, Foster City, California, USA) and the nucleotide sequences were determined using Sanger sequencing.

3.3.6 Construction of mutant viruses

The amino acid residues at positions 385, 581, and 934 in the M segment of Tk-F123 and Ng-F264 were swapped individually via site-directed mutagenesis using KOD One PCR Master Mix (Toyobo, Osaka, Japan) and primers containing the mutation. Three plasmids containing point mutations in Gn and Gc were constructed based on Tk-F123 and four plasmids were based on Ng-F264. These plasmids were validated by sequencing and then co-transfected into BSR T7/5 cells as previously described. Mutant viruses were rescued and examined using a previously outlined method (Wulandari et al., 2024). All viruses were passaged in Vero E6 cells and stored at -80°C.

3.3.7 Quantification of viral RNA

The spleens, lungs, kidneys, and brains of SFTSV-infected mice were homogenized in phosphate-buffered saline using a TOMY Micro Smash MS-100 (TOMY Digital Biology Co., Ltd., Tokyo, Japan) and total RNA was extracted using ISOGEN II (Nippon Gene Co., Ltd, Toyama, Japan). Viral RNA copy numbers were determined by quantitative real-time RT-PCR (qRT-PCR), as described in our previous reports (Ando et al., 2021; Hayasaka et al., 2015), using an L segment based on the RdRp-SFTSV-specific primer set. Real-time PCR was performed using a One-Step PrimeScript RT-PCR Kit (Takara Bio Inc., Shiga, Japan) and a CFX96 Touch real-time PCR detection system (Bio-Rad, Hercules, CA, USA). Copy numbers were calculated as the ratio of copy numbers to those of standard controls. Standard SFTSV RNA was prepared from a cloned plasmid containing a previously described RdRp insert generated using RT-PCR (Ando et al., 2021; Hayasaka et al., 2015).

3.3.8 Three-dimensional structures of glycoprotein SFTSV

The three-dimensional structures of Tk-F123 and Ng-F264 were predicted using the I-TASSER software. Based on previous structural studies, a Protein Data Bank (PDB) model of the glycoprotein from SFTSV (PDB code: 8ILQ) (Du et al., 2023) was obtained from the PDB database and used to visualize identified mutations using MODELLER software (Sali and Blundell, 1993).

3.3.9 Statistical analysis

One-way ANOVA with Tukey's multiple comparison test (* $P < 0.05$). All statistical tests were performed using R version 4.2.2.

3.4 RESULTS

3.4.1 Lethality of A129 mice infected with SFTSV Tk-F123 and Ng-F264 strains

In preliminary experiments, we examined the pathogenicity of SFTSV isolates from cat samples in A129 mice (data not shown). Among them, we selected two cat-derived SFTSV strains, Tk-F123 and Ng-F264, which showed high and low lethality, respectively, in mice. Subcutaneous infection with Tk-F123 resulted in 100% fatality (Fig. 3.1.A) in A129 mice following weight reduction (Fig. 3.1.B). In contrast, Ng-F264-infected mice did not show any apparent weight reduction, and all mice survived (Fig. 3.1.A and 3.1.B). These results indicate that Ng-F264 caused significantly lower virulence than Tk-F123 in A129 mice.

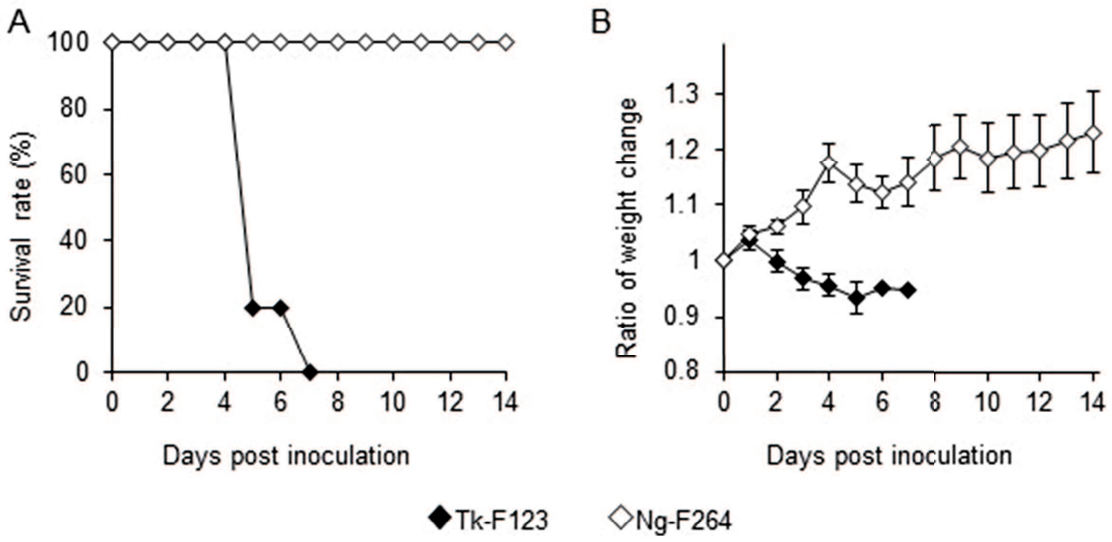

Fig. 3.1 Virulence of SFTSV Tk-F123 and Ng-F264 strains in A129 mice. Survival curves (A) and body weight ratios (B) of A129 mice subcutaneously infected with 104 FFU of Tk-F123 and Ng-F264 (n = 5). Error bars indicate the standard errors.

3.4.2 Nucleotides differences and amino acid sequences between Tk-F123 and Ng-F264

We compared the viral gene sequences of the strains Tk-F123 and Ng-F264. There were 5, 10, and 19 nucleotide differences in the S, M, and L segments, between Tk-F123 and Ng-F264, respectively (Table 3.1). Differences in three amino acids were observed between structural proteins in the M segment of them (Table 3.1). In contrast, no amino acid differences were observed in the S and L segments between Tk-F123 and Ng-F264 (Table 3.1), indicating that viral nucleocapsids, NSs, and RdRp are unlikely to contribute to the different virulence of Tk-F123 and Ng-F264. Therefore, we predicted that the M segment predominantly contribute to the differential virulence of Tk-F123 and Ng-F264 in A129 mice, and focused on the three amino acid differences in Gn and Gc following a series of experiments using reassortant and point-mutated viruses.

Table 3.1 Nucleotide differences between SFTSV Tk-F123 and Ng-F264 strains.

Segment	Protein	Nucleotide			Amino acid		
		position	Tk-F123	Ng-F264	position	Tk-F123	Ng-F264
S	NP	317	C	T	106	Leu	Leu
		673	T	C	224	Phe	Phe
	NSs	1196	A	T	183	Ile	Ile
		1376	A	G	123	Ala	Ala
		1418	C	T	109	Arg	Arg
M	Gn	1171	A	G	385	Thr	Ala
		1344	G	A	442	Leu	Leu
	Gc	1759	G	A	581	Gly	Arg
		1887	G	A	623	Lys	Lys
		2070	C	T	684	Phe	Phe
		2088	A	T	690	Gly	Gly
		2691	A	G	891	Ser	Ser
		2819	G	A	934	Ser	Asn
		3147	T	C	1043	Val	Val
	3’ UTR	3251	C	T	-	-	-
L	RdRp	88	T	C	29	Tyr	Tyr
		160	T	C	53	Asp	Asp
		778	A	G	259	Glu	Glu
		1045	A	G	348	Ser	Ser
		1106	T	C	369	Leu	Leu
		1126	A	G	375	Leu	Leu
		1402	C	T	467	Phe	Phe
		1720	A	G	573	Leu	Leu
		1837	A	G	612	Thr	Thr
		2389	A	G	796	Gly	Gly
		2437	A	G	812	Arg	Arg
		3985	T	C	1328	Tyr	Tyr
		4378	T	C	1459	Gly	Gly
		4669	C	T	1556	Asp	Asp
		4945	A	G	1648	Glu	Glu
		5014	C	T	1671	Ile	Ile
		5470	C	T	1823	Leu	Leu
		5554	C	T	1851	Asn	Asn
		6088	A	G	2020	Ala	Ala

3.4.3 M segment is responsible for the distinct virulence between Tk-F123 and Ng-F264

To confirm whether the M segments of the Tk-F123 and Ng-F264 strains contributed to the differences in pathogenicity, we first constructed reassortant viruses that switched to a single M segment (Fig. 3.2.A) and examined their virulence in A129 mice. rNg-F264$_{M123}$ showed 100% lethality (Fig. 3.2.B) following weight reduction (Fig. 3.2.C) as similar as rTk-F123. In contrast, rTk-F123$_{M264}$ caused no fatalities or weight reduction in mice, similar to rNg-F264 (Fig. 3.2.B and 3.2.C). These observations indicated that the M segments of Tk-F123 and Ng-F264 determine fatal and non-fatal infections, respectively, in A129 mice.

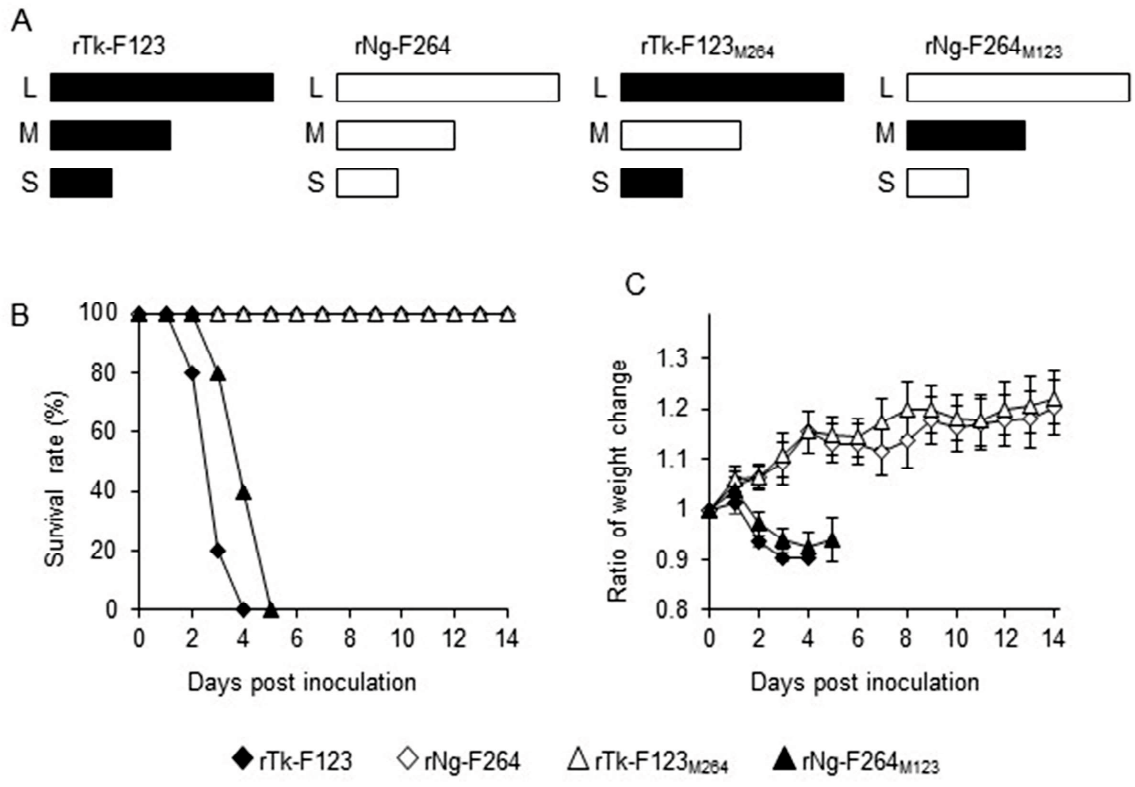

Fig. 3.2 Virulence of reassortant viruses switching the M segment of Tk-F123 and Ng-F264 strains. (A) Schematic representation of SFTSV reassortant viruses generated using reverse genetics. Black and white boxes indicate the segments of Tk-F123 and F264, respectively. Survival curves (B) and body weight ratios (C) of A129 mice subcutaneously infected with 10^4 FFU of the recombinant viruses (n = 5). Error bars indicate the standard errors.

3.4.4 Two amino acids in Gc proteins contribute to the different virulence in A129 mice

Next, we examined the amino acid residues in the M segment that influence virulence in mice. Three amino acid differences were observed in the M segment, one in Gn, and two in Gc (Table 3.1). Therefore, we constructed a point-mutated SFTSV based on Tk-F123 and Ng-F264 (Fig. 3.3.A).

rTk-F123-Gn_{385A} of the Tk-F123-based virus showed 100% fatality (Fig. 3.3.B) after significant weight reduction (Fig. 3.3.C), similar to the parent rTk-F123, indicating that this amino acid position does not influence virulence. rTk-F123-Gc_{581R} and rTk-F123-Gc_{934N} did not exhibit any apparent weight loss and all mice survived (Fig. 3.3.B and 3.3.C).

In contrast, any Ng-F264-based viruses, rNg-F264-Gn_{385T}, rNg-F264-Gc_{581G}, and rNg-F264-Gc_{934S}, showed no fatality (Fig. 3.3.B) and weight loss (Fig. 3.3.C) in mice as the same as parent rNg-F264. These observations imply that single amino acid substitutions are not responsible for the high virulence of Tk-F123 but suggest that a pair of amino acid substitutions, glycine at residue 581 (581G) and serine at residue 934 (934S) in the Gc protein, contribute to fatal infection in mice.

To confirm the virulence of these two amino acids, we constructed rNg-F264-$Gc_{581G-934S}$, including two substitutions based on Ng-F264 (Fig. 3.3.A). rNg-F264-$Gc_{581G-934S}$ caused 100% fatality (Fig. 3.3.B) and weight reduction (Fig. 3.3.C) in A129 mice, similar to rTk-F123, indicating that the glycine and serine pair in the Gc protein is responsible for the fatal infection.

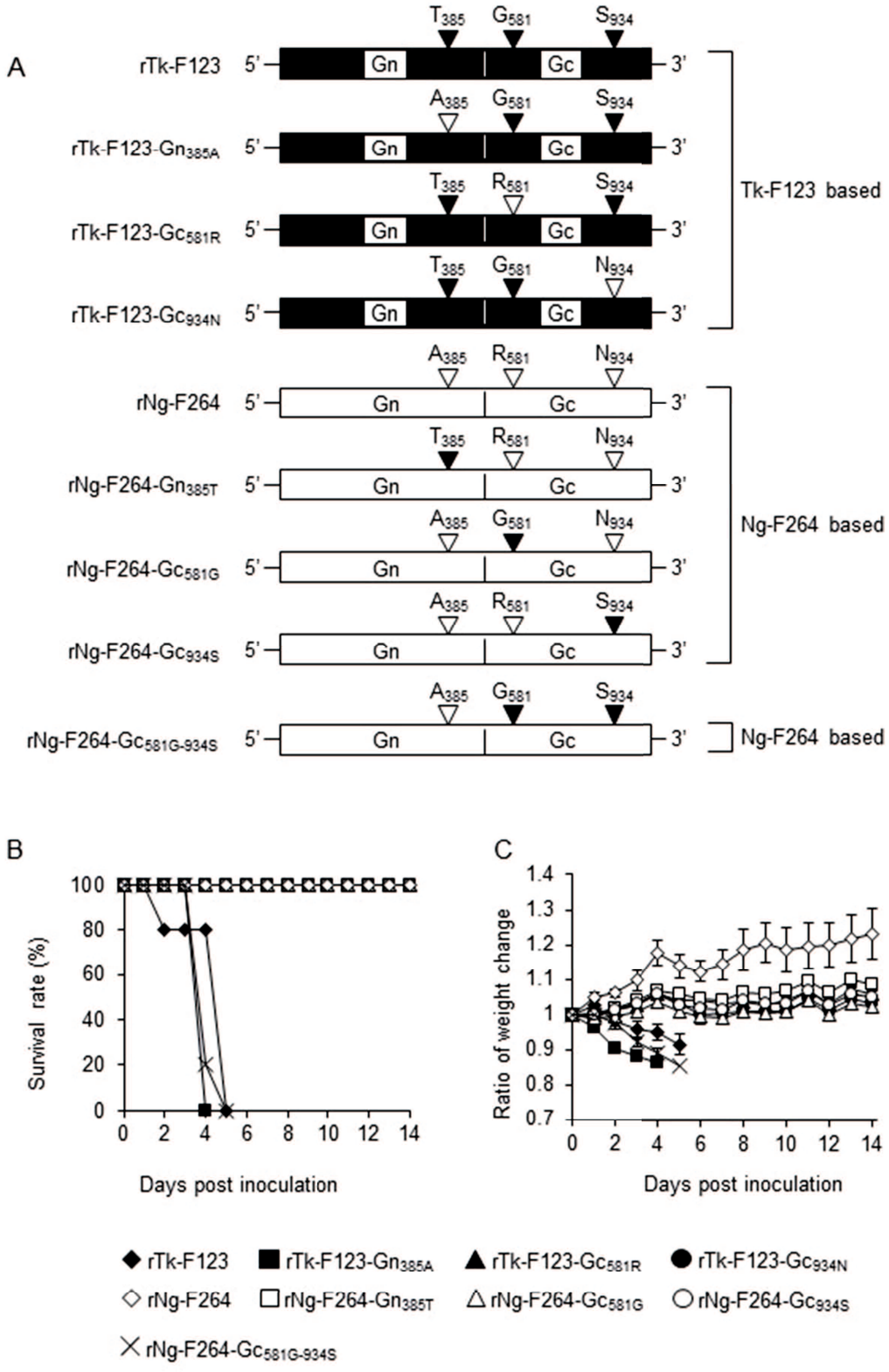

Fig. 3.3 Virulence of point-mutated viruses in the Gn and Gc proteins based on Tk-F123 and Ng-F264 strains. (A) Schematic representation of the construction of SFTSV mutant viruses using reverse genetics. Black and white boxes indicate the segments of Tk-F123 and F264, respectively. (B) Survival curves and (C) body weight ratios of A129 mice subcutaneously infected with 104 FFU of the recombinant viruses (n = 5). Error bars indicate the standard errors.

3.4.5 Viral loads in mice

In accordance with our previous study (Shimada et al., 2015), we examined viral RNA levels in the lungs, spleen, liver, kidney, and brain of mice infected with virulent Tk-F123, rNg-F264$_{M123}$, and rNg-F264-Gc$_{581G-934}$ and avirulent rNg-F264 and rTk-F123$_{M264}$ at 3 dpi (Fig. 3.4). Viral RNAs were detected in all mice infected with virulent and avirulent strains (Fig. 3.4). Although statistically significant differences were observed between a few samples, viral RNA levels of the virulent types tended to be higher than those of the avirulent types in the lungs, spleen, kidneys, and brain (Fig.3.4). These results suggested that the Gc protein, including the glycine-serine pair, has the functional property of high viral replication, which contributes to high virulence.

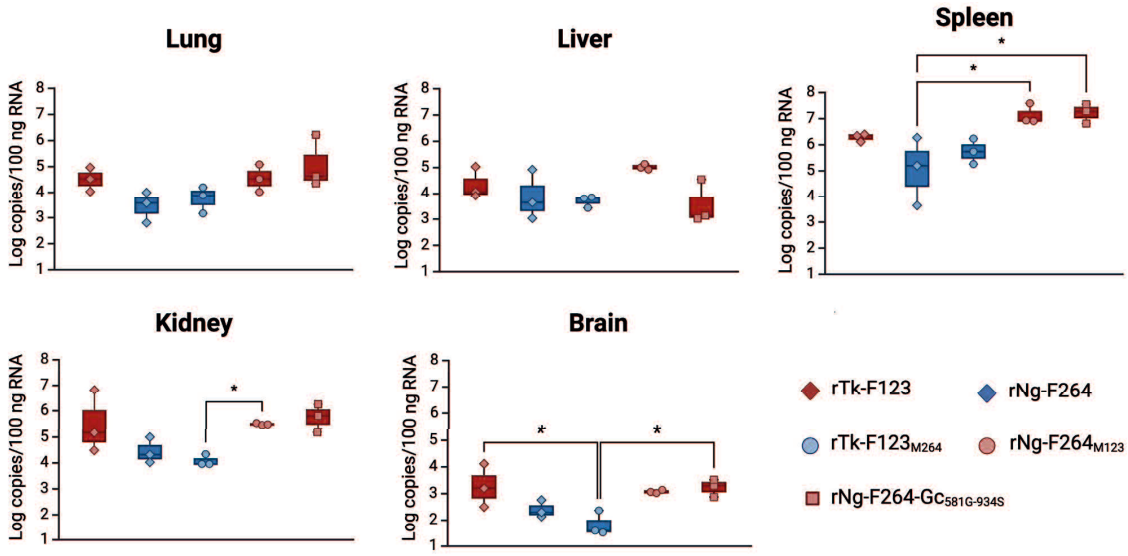

Figure 3.4 Viral RNA copy numbers in tissues of SFTSV-infected mice. RNAs were extracted from the lung, spleen, liver, kidney, and brain of mice infected with rTk-F123, rNg-F264, rTk-F123$_{M264}$, rNg-F264$_{M123}$, and rNg-F264-Gc$_{581G-934S}$ at 3 dpi, and viral RNA copy numbers were assessed with real-time PCR (n = 3 per group). The asterisks indicate significance compared to each virus-infected mouse sample analysed by one-way Analysis of Variance with Tukey multiple comparisons test (*P $\leq$ 0.05).

3.5 Discussion

In this study, we compared the virulence of SFTSV using reassortant and point-mutated recombinant viruses based on virulent Tk-F123 and avirulent Ng-F264 in A129 mice and identified a pair of amino acid residues in the Gc protein, glycine residue 581 (G_{581}) and serine residue 934 (S_{934}) of Tk-F123, leading to a fatal infection. Gc exists as a heterodimer with Gn and forms pentameric and hexameric structures on the viral surface (Du et al., 2023). This assembly stabilizes Gc in a metastable pre-fusion conformation and functions as a fusion protein. Our findings suggest that this pair of residues affects the Gc protein function and regulates SFTSV virulence *in vivo*.

To gain structural insight into amino acid residues 581 and 934 in the Gc proteins of Tk-F123 and Ng-F264, respectively, we constructed structural analysis models of Gc (Fig. 3.5). These two residues are located close to the protein surface. Residue 581 significantly affected the cellular localization of proteins (Doron-Mandel et al., 2021). The arginine residue 581 (R_{581}) of Ng-F264 possesses a positively charged side chain, whereas G_{581} of Tk-F123 lacks a side chain. G_{581} appeared to provide more conformational flexibility to the protein backbone than did R_{581} (Fig. 3.5). These predictions suggest that different amino acid properties potentially destabilize protein folding and are likely associated with a shift in the cellular localization of the Gc glycoprotein, potentially affecting its function.

A previous study reported that the lack of N-linked glycosylation of the Gc protein reduced the pathogenicity of SFTSV (Shimojima et al., 2024). Asparagine residue 936 is an N-linked glycosylation site in the GPs of SFTSV. S_{934} and N_{934} are close to this site, raising the possibility that different residues may affect the efficiency of glycosylation at this site. In addition, S_{934} and N_{934} are polar uncharged residues; however, N_{934} is slightly larger than S_{934}, which may affect protein function. Overall, the

differences in residues 581 and 934 in the Gc protein may lead to the pathogenic outcomes that affect virulence factors in mice.

According to published sequences of SFTSV strains, most SFTSV strains possess a virulent pair of G_{581} and S_{934} (Tk-F123 type) in the Gc protein, indicating that virulent type strains seem to be isolated from both of fatal and recovered cases. Some strains possessed either R581 or N934 amino acids (Ng-F264 type), and only the Tk-F123 and NFe111 strains found in our previous study (Ando et al., 2021) possessed avirulent pairs of R_{581} and N_{934}. In a previous study, we compared the pathogenicity of 11 SFTSV strains isolated from fatal and recovered A129 mice and we found that NFe111 exhibited no fatality (Ando et al., 2021). The other 10 strains showed 20–100% fatality, and these amino acids were the virulent types of G_{581} and S_{934} (Ando et al., 2021). Although the fate of Ng-F264-derived cats is unknown, NFe111 has been isolated from recovered cats, implying that the R_{581} and N_{934} residues of NFe111 may cause low pathogenicity in cats. The findings suggest that SFTSV fundamentally possesses virulent types of G_{581} and S_{934} in the Gc and has intrinsic properties of high pathogenicity. However, discussing whether the virulent R_{581} and N_{934} pair is a critical factor in high pathogenicity in humans and cats is difficult because virulent amino acid types have been identified not only in fatal cases but also in most recovered cases. Alternatively, the avirulent R_{581} and N_{934} strains are present in nature and may lead to relatively mild disease. Therefore, investigating the distribution of avirulence types in endemic areas would be interesting.

Ng-F264 infection did not result in apparent weight reduction or fatality in mice; however, viral replication was observed in the body using viral RNA detection. Viral copy numbers tended to be lower in mice infected with R_{581} and N_{934}-type viruses than in mice infected with G_{581} and S_{934}-type viruses. A129 mice are IFN-I response deficient; therefore, innate immunity does not influence viral replication. In addition, fatal mice

died at 2–6 dpi, indicating that the acquired immunity was not affected considerably. Therefore, viral replication and propagation at the cellular level may contribute to the different virulence of Tk-F123 and Ng-F264.

Pathogenicity and fatality due to SFTSV infections seem to be associated with multiple mechanisms such as viral replication in infected cells and the host immune response. In our preliminary experiments, Tk-F123 exhibited significantly higher viral yields than Ng-F264 in some cell lines, such as monkey-derived Vero E6 cells (data not shown), suggesting that amino acid substitutions in the Gc protein may affect viral replication *in vitro*. However, our unpublished data show that the infectivity, replication, and production of SFTSV depend on the cell types derived from different animal species and tissues, suggesting that viral propagation in some cell lines may not reflect to high pathogenicity in mice. Therefore, further elucidation of the mechanism *in vitro* using cells derived from several animal species, including mice, cats, and humans, will provide important information for elucidating the mechanism of viral replication associated with high pathogenicity *in vivo*.

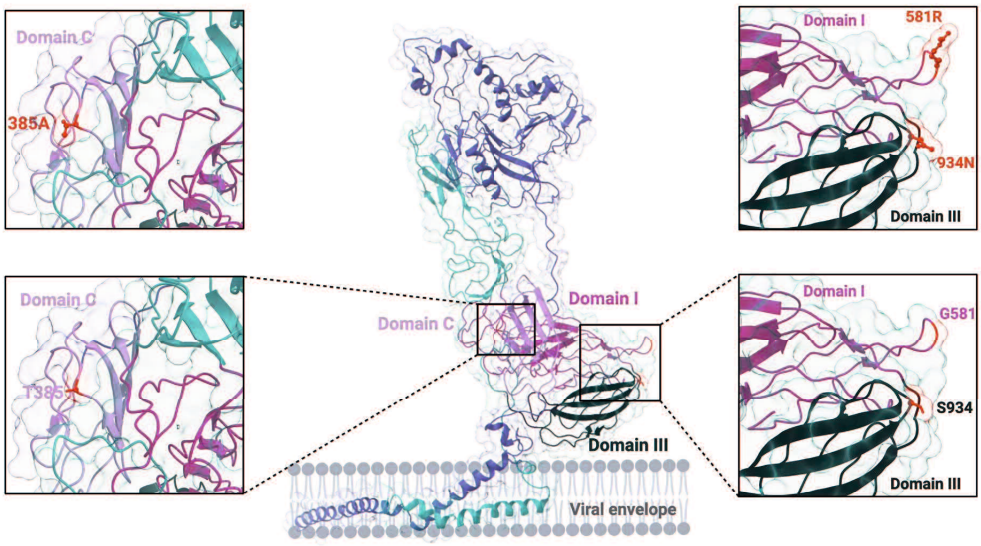

Figure 3.5 Structural models of glycoprotein SFTSV: Evaluation of the amino acids at positions 385 in Gn, 581, and 934 in Gc.

3.6 Conclusions

In conclusion, we identified a pair of amino acid residues, G_{581} and S_{934}, in the Gc protein that led to fatal infection. Our findings of amino acid substitutions highlight the importance of Gc as a virulence factor of SFTSV, along with the previously recognized NSs protein. The Gc protein may be a key target for vaccine design as it plays a crucial role in SFTSV virulence and pathogenesis. Therefore, elucidating the attenuation mechanism by focusing on the avirulent types of R_{581} and N_{934} types would provide useful clues for the development of effective live-attenuated vaccines and antiviral strategies. The findings enhance our understanding of SFTSV pathogenesis, immune responses, and antiviral strategies.

4. General Conclusion

Trisegmented bunyaviruses constitute a category of viruses within the *Bunyavirales* order, distinguished by their segmented, negative-sense RNA genomes that are encoded in an orientation opposite to that of messenger RNA. Their members infect broad ranges of hosts, including several significant human pathogens. Reverse genetic systems have been essential in the investigation of trisegmented bunyaviruses. The process of introducing a precise genetic change into a viral genome, known as viral reverse genetics, has revolutionized our understanding of negative-sense, segmented RNA viruses. While the specific characteristics of reverse genetic systems vary among different viruses, the fundamental principles of biology remain the same. Here, we examine the development of reverse genetic systems as applied to these virus members, emphasizing conserved approaches illustrated by some of the prominent members that cause significant human disease. We also describe the utility of their genetic systems in the determination of the responsible gene for the enhanced virulence of trisegmented bunyaviruses.

Despite extensive geographical distribution and substantial populations susceptible to Bunyavirus infections, significant knowledge gaps remain regarding the host and viral factors that influence the pathogenesis of Bunyavirus, particularly TFLV and SFTSV. Further exploration of the function of viral proteins is necessary, and developments in molecular virology tools and improved small-animal models will lead to significant mechanistic understanding of Bunyavirus pathogenesis. It is essential to mitigate the impact of Bunyavirus infections on patients and public health systems by developing rapid and reliable diagnostics, effective vaccinations, and antiviral treatments. Vaccines may protect against bunyaviruses in ways other than classical antibody-mediated neutralization. Studying how vaccines protect against the Bunyavirus

group will help us understand how the host can control the infection and help us come up with treatment plans that boost immune responses while limiting immunopathology. Molecular virology, immunology, vaccinology, entomology, veterinary health, and public health will collectively need to continue their contributions to address the substantial risk of Bunyavirus group infection and disease in endemic areas.

In conclusion, we were able to rescue recombinant TFLV and SFTSV from cDNA clones, allowing detailed studies on viral genetics and pathogenesis. We also describe the molecular determinants of virulence in SFTSV, which is crucial for developing effective vaccines and therapeutics. Finally, we highlight that reverse genetics continues to be a powerful tool in elucidating the molecular mechanisms of virulence in trisegmented bunyaviruses, which will contribute to our understanding of viral biology, pathogenesis, and intervention strategies.

ACKNOWLEDGEMENT

Words cannot express my gratitude to my professor and chair of committee, **Prof. Daisuke HAYASAKA, DVM., Ph.D.** (Professor in Veterinary Microbiology, Joint Faculty of Veterinary Medicine, Yamaguchi University), for providing me invaluable opportunity, guidance, patience, and feedback. I could not have undertaken this journey without his continuous and unwavering support.

I would like to express my deepest gratitude to my defense committee, **Assoc. Prof. Yuusuke MATSUMOTO, DVM., Ph.D** (Joint Faculty of Veterinary Medicine, Kagoshima University), **Prof. Ai TAKANO, DVM., Ph.D., Prof. Takuya MIZUNO, DVM., Ph.D.,** and **Assoc. Prof. Hiroshi SHIMODA, DVM., Ph.D.** (Joint Faculty of Veterinary Medicine, Yamaguchi University), who generously provided knowledge and expertise.

I would like to extend my sincere gratitude to the Dean and all vice deans, the head of division, and the members of Department of Health, Faculty of Vocational Studies, Universitas Airlangga, for all their help and positive support until I achieve my goal. Many thanks to all members of Veterinary Microbiology Laboratory, Joint Faculty of Veterinary Medicine, Yamaguchi University, for making me comfortable and joyful during my days in laboratory.

Finally, I would like to express my deepest appreciation to my best support system: **my mother, my father, my husband, Asst. Prof. Oky Setyo Widodo, DVM, M.Sc., Ph.D.,** and **my daughter, Sybill.** Thank you so much for all the sacrifices to allow me to continue studying until I received my PhD.

REFERENCES

Abudurexiti, A., Adkins, S., Alioto, D., Alkhovsky, S. V., Avšič-Županc, T., Ballinger, M. J., Bente, D. A., Beer, M., Bergeron, É., Blair, C. D., Briese, T., Buchmeier, M. J., Burt, F. J., Calisher, C. H., Cháng, C., Charrel, R. N., Choi, I. R., Clegg, J. C. S., De La Torre, J. C., . . . Zhāng, Y. (2019). Taxonomy of the order Bunyavirales: update 2019. Archives of Virology, 164(7), 1949–1965. https://doi.org/10.1007/s00705-019-04253-6

Ando, T., Nabeshima, T., Inoue, S., Tun, M. M. N., Obata, M., Hu, W., Shimoda, H., Kurihara, S., Izumikawa, K., Morita, K., & Hayasaka, D. (2021). Severe Fever with Thrombocytopenia Syndrome in Cats and Its Prevalence among Veterinarian Staff Members in Nagasaki, Japan. Viruses, 13(6), 1142. https://doi.org/10.3390/v13061142

Barker, J., daSilva, L. L. P., & Crump, C. M. (2023). Mechanisms of bunyavirus morphogenesis and egress. Journal of General Virology, 104(4). https://doi.org/10.1099/jgv.0.001845

Barton, L. L., Mets, M. B., & Beauchamp, C. L. (2002). Lymphocytic choriomeningitis virus: Emerging fetal teratogen. American Journal of Obstetrics and Gynecology, 187(6), 1715–1716. https://doi.org/10.1067/mob.2002.126297

Begum, F., Wisseman, C. L., & Casals, J. (1970). Tick-Borne Viruses Of West Pakistan: Ii. Hazara Virus, A New Agent Isolated From Ixodes Redikorzeviticks From The Kaghan Valley, W. Pakistan12. *American Journal of Epidemiology*, *92*(3), 192–194. https://doi.org/10.1093/oxfordjournals.aje.a121197

Bergeron, E., AlbariñO, C. G., Khristova, M. L., & Nichol, S. T. (2009). Crimean-Congo Hemorrhagic Fever Virus-Encoded Ovarian Tumor Protease Activity Is Dispensable for Virus RNA Polymerase Function. *Journal of Virology*, *84*(1), 216–226. https://doi.org/10.1128/jvi.01859-09

Bergeron, É., Zivcec, M., Chakrabarti, A. K., Nichol, S. T., Albariño, C. G., & Spiropoulou, C. F. (2015). Recovery of Recombinant Crimean Congo Hemorrhagic Fever Virus Reveals a Function for Non-structural Glycoproteins Cleavage by Furin. *PLoS Pathogens*, *11*(5), e1004879. https://doi.org/10.1371/journal.ppat.1004879

Billecocq, A., Gauliard, N., May, N. L., Elliott, R. M., Flick, R., & Bouloy, M. (2008). RNA polymerase I-mediated expression of viral RNA for the rescue of infectious virulent and avirulent Rift Valley fever viruses. *Virology*, *378*(2), 377–384. https://doi.org/10.1016/j.virol.2008.05.033

Bird, B. H., AlbariñO, C. G., Hartman, A. L., Erickson, B. R., Ksiazek, T. G., & Nichol, S. T. (2008). Rift Valley Fever Virus Lacking the NSs and NSm Genes Is Highly Attenuated, Confers Protective Immunity from Virulent Virus Challenge, and Allows for Differential Identification of Infected and Vaccinated Animals. Journal of Virology, 82(6), 2681–2691. https://doi.org/10.1128/jvi.02501-07

Blakqori, G., & Weber, F. (2005). Efficient cDNA-Based Rescue of La Crosse Bunyaviruses Expressing or Lacking the Nonstructural Protein NSs. Journal of Virology, 79(16), 10420–10428. https://doi.org/10.1128/jvi.79.16.10420-10428.2005

Boshra, H. (2022). An Overview of the Infectious Cycle of Bunyaviruses. Viruses, 14(10), 2139. https://doi.org/10.3390/v14102139

Bouloy, M., & Flick, R. (2009). Reverse genetics technology for Rift Valley fever virus: Current and future applications for the development of therapeutics and vaccines. Antiviral Research, 84(2), 101–118. https://doi.org/10.1016/j.antiviral.2009.08.002

Brennan, B., Li, P., Zhang, S., Li, A., Liang, M., Li, D., & Elliott, R. M. (2015). Reverse Genetics System for Severe Fever with Thrombocytopenia Syndrome Virus. Journal of Virology, 89(6), 3026–3037. https://doi.org/10.1128/jvi.03432-14

Bridgen, A., & Elliott, R. M. (1996). Rescue of a segmented negative-strand RNA virus entirely from cloned complementary DNAs. Proceedings of the National Academy of Sciences, 93(26), 15400–15404. https://doi.org/10.1073/pnas.93.26.15400

Brocato, R. L., & Hooper, J. W. (2019). Progress on the Prevention and Treatment of Hantavirus Disease. Viruses, 11(7), 610. https://doi.org/10.3390/v11070610

Bryden, S. R., Dunlop, J. I., Clarke, A. T., Fares, M., Pingen, M., Wu, Y., Willett, B. J., Patel, A. H., Gao, G. F., Kohl, A., & Brennan, B. (2022). Exploration of immunological responses underpinning severe fever with thrombocytopenia syndrome virus infection reveals IL-6 as a therapeutic target in an immunocompromised mouse model. PNAS Nexus, 1(1). https://doi.org/10.1093/pnasnexus/pgac024

Buchholz, U. J., Finke, S., & Conzelmann, K. K. (1999). Generation of Bovine Respiratory Syncytial Virus (BRSV) from cDNA: BRSV NS2 Is Not Essential for Virus Replication in Tissue Culture, and the Human RSV Leader Region Acts as a Functional BRSV Genome Promoter. Journal of Virology, 73(1), 251–259. https://doi.org/10.1128/jvi.73.1.251-259.1999

Burt, F. J., Spencer, D. C., Leman, P. A., Patterson, B., & Swanepoel, R. (1996). Investigation of tick-borne viruses as pathogens of humans in South Africa and evidence of Dugbe virus infection in a patient with prolonged thrombocytopenia. *Epidemiology and Infection*, *116*(3), 353–361. https://doi.org/10.1017/s0950268800052687

Carter, S. D., Surtees, R., Walter, C. T., Ariza, A., Bergeron, É., Nichol, S. T., Hiscox, J. A., Edwards, T. A., & Barr, J. N. (2012). Structure, Function, and Evolution of the Crimean-Congo Hemorrhagic Fever Virus Nucleocapsid Protein. *Journal of Virology*, *86*(20), 10914–10923. https://doi.org/10.1128/jvi.01555-12

Casel, M. A., Park, S. J., & Choi, Y. K. (2021). Severe fever with thrombocytopenia syndrome virus: emerging novel phlebovirus and their control strategy.

Experimental & Molecular Medicine, 53(5), 713–722. https://doi.org/10.1038/s12276-021-00610-1

Davies F. G. (1997). Nairobi sheep disease. Parassitologia, 39(2), 95–98.

Doron-Mandel, E., Koppel, I., Abraham, O., Rishal, I., Smith, T. P., Buchanan, C. N., Sahoo, P. K., Kadlec, J., Oses-Prieto, J. A., Kawaguchi, R., Alber, S., Zahavi, E. E., Di Matteo, P., Di Pizio, A., Song, D., Okladnikov, N., Gordon, D., Ben-Dor, S., Haffner-Krausz, R., . . . Fainzilber, M. (2021). The glycine arginine-rich domain of the RNA-binding protein nucleolin regulates its subcellular localization. The EMBO Journal, 40(20). https://doi.org/10.15252/embj.2020107158

Dowall, S. D., Findlay-Wilson, S., Rayner, E., Pearson, G., Pickersgill, J., Rule, A., Merredew, N., Smith, H., Chamberlain, J., & Hewson, R. (2011). Hazara virus infection is lethal for adult type I interferon receptor-knockout mice and may act as a surrogate for infection with the human-pathogenic Crimean–Congo hemorrhagic fever virus. *Journal of General Virology*, *93*(3), 560–564. https://doi.org/10.1099/vir.0.038455-0

Du, S., Peng, R., Xu, W., Qu, X., Wang, Y., Wang, J., Li, L., Tian, M., Guan, Y., Wang, J., Wang, G., Li, H., Deng, L., Shi, X., Ma, Y., Liu, F., Sun, M., Wei, Z., Jin, N., . . . Li, C. (2023). Cryo-EM structure of severe fever with thrombocytopenia syndrome virus. Nature Communications, 14(1). https://doi.org/10.1038/s41467-023-41804-7

Dunn, E. F., Pritlove, D. C., Jin, H., & Elliott, R. M. (1995). Transcription of a Recombinant Bunyavirus RNA Template by Transiently Expressed Bunyavirus Proteins. Virology, 211(1), 133–143. https://doi.org/10.1006/viro.1995.1386

Elaldi, N., Bodur, H., Ascioglu, S., Celikbas, A., Ozkurt, Z., Vahaboglu, H., Leblebicioglu, H., Yilmaz, N., Engin, A., Sencan, M., Aydin, K., Dokmetas, I., Cevik, M. A., Dokuzoguz, B., Tasyaran, M. A., Ozturk, R., Bakir, M., & Uzun, R. (2009). Efficacy of oral ribavirin treatment in Crimean-Congo haemorrhagic fever: A quasi-experimental study from Turkey. *Journal of Infection*, *58*(3), 238–244. https://doi.org/10.1016/j.jinf.2009.01.014

Elliott, R. M. (1990). Molecular biology of the Bunyaviridae. *Journal of General Virology*, *71*(3), 501–522. https://doi.org/10.1099/0022-1317-71-3-501

Elliott, R. M. (2014). Orthobunyaviruses: recent genetic and structural insights. Nature Reviews Microbiology, 12(10), 673–685. https://doi.org/10.1038/nrmicro3332
Ergönül, O. (2006). Crimean-Congo haemorrhagic fever. *The Lancet Infectious Diseases*, *6*(4), 203–214. https://doi.org/10.1016/s1473-3099(06)70435-2

Feng, K., Ushie, B. B., Zhang, H., Li, S., Deng, F., Wang, H., & Ning, Y. (2024). Pathogenesis and virulence of Heartland virus. Virulence, 15(1). https://doi.org/10.1080/21505594.2024.2348252

Flick, K., Hooper, J. W., Schmaljohn, C. S., Pettersson, R. F., Feldmann, H., & Flick, R. (2003). Rescue of hantaan virus minigenomes. Virology, 306(2), 219–224. https://doi.org/10.1016/s0042-6822(02)00070-3

Flick, R., & Pettersson, R. F. (2001). Reverse Genetics System for Uukuniemi Virus (Bunyaviridae): RNA Polymerase I-Catalyzed Expression of Chimeric Viral RNAs. Journal of Virology, 75(4), 1643–1655. https://doi.org/10.1128/jvi.75.4.1643-1655.2001

Flick, R., Flick, K., Feldmann, H., & Elgh, F. (2003). Reverse Genetics for Crimean-Congo Hemorrhagic Fever Virus. *Journal of Virology*, *77*(10), 5997–6006. https://doi.org/10.1128/jvi.77.10.5997-6006.2003

Freitas, N., Enguehard, M., Denolly, S., Levy, C., Neveu, G., Lerolle, S., Devignot, S., Weber, F., Bergeron, E., Legros, V., & Cosset, F. (2020). The interplays between Crimean-Congo hemorrhagic fever virus (CCHFV) M segment-encoded accessory proteins and structural proteins promote virus assembly and infectivity. *PLoS Pathogens*, *16*(9), e1008850. https://doi.org/10.1371/journal.ppat.1008850

Fu, Y., Li, S., Zhang, Z., Man, S., Li, X., Zhang, W., Zhang, C., & Cheng, X. (2016). Phylogeographic analysis of severe fever with thrombocytopenia syndrome virus from Zhoushan Islands, China: implication for transmission across the ocean. Scientific Reports, 6(1). https://doi.org/10.1038/srep19563

Fuller, J., Surtees, R. A., Slack, G. S., Mankouri, J., Hewson, R., & Barr, J. N. (2019). Rescue of Infectious Recombinant Hazara Nairovirus from cDNA Reveals the Nucleocapsid Protein DQVD Caspase Cleavage Motif Performs an Essential Role other than Cleavage. *Journal of Virology*, *93*(15). https://doi.org/10.1128/jvi.00616-19

Gargili, A., Estrada-Peña, A., Spengler, J. R., Lukashev, A., Nuttall, P. A., & Bente, D. A. (2017). The role of ticks in the maintenance and transmission of Crimean-Congo hemorrhagic fever virus: A review of published field and laboratory studies. *Antiviral Research*, *144*, 93–119. https://doi.org/10.1016/j.antiviral.2017.05.010

Garrison, A. R., Владимирович, S. V. a. [. C., Avšič-Županc, T., Bente, D. A., Bergeron, É., Burt, F., Di Paola, N., Ergünay, K., Hewson, R., Kuhn, J. H., Mirazimi, A., Παπά, A. P. [., Sall, A. A., Spengler, J. R., Palacios, G., & Consortium, I. R. (2020). ICTV Virus Taxonomy Profile: Nairoviridae. *Journal of General Virology*, *101*(8), 798–799. https://doi.org/10.1099/jgv.0.001485

Genus: Bandavirus | ICTV. (n.d.). https://ictv.global/report/chapter/phenuiviridae/phenuiviridae/bandavirus

Guu, T. S. Y., Zheng, W., & Tao, Y. J. (2011). Bunyavirus: Structure and Replication. Advances in Experimental Medicine and Biology, 245–266. https://doi.org/10.1007/978-1-4614-0980-9_11

Habjan, M., Penski, N., Spiegel, M., & Weber, F. (2008). T7 RNA polymerase-dependent and -independent systems for cDNA-based rescue of Rift Valley fever virus. Journal of General Virology, 89(9), 2157–2166. https://doi.org/10.1099/vir.0.2008/002097-0

Hartman, A. L., & Myler, P. J. (2023). Bunyavirales: Scientific Gaps and Prototype Pathogens for a Large and Diverse Group of Zoonotic Viruses. The Journal of Infectious Diseases, 228(Supplement_6), S376–S389. https://doi.org/10.1093/infdis/jiac338

Hawman, D. W., & Feldmann, H. (2023). Crimean–Congo haemorrhagic fever virus. Nature Reviews Microbiology, 21(7), 463–477. https://doi.org/10.1038/s41579-023-00871-9

Hayasaka, D., Shimada, S., Aoki, K., Takamatsu, Y., Uchida, L., Horio, M., Fuxun, Y., & Morita, K. (2015). Epidemiological Survey of Severe Fever with Thrombocytopenia Syndrome Virus in Ticks in Nagasaki, Japan. Tropical Medicine and Health, 43(3), 159–164. https://doi.org/10.2149/tmh.2015-01

Horne, K., & Vanlandingham, D. (2014). Bunyavirus-Vector Interactions. Viruses, 6(11), 4373–4397. https://doi.org/10.3390/v6114373

Hu, Q., Zhang, Y., Jiang, J., & Zheng, A. (2023). Two Point Mutations in the Glycoprotein of SFTSV Enhance the Propagation Recombinant Vesicular Stomatitis Virus Vectors at Assembly Step. Viruses, 15(3), 800. https://doi.org/10.3390/v15030800

Hulswit, R. J. G., Paesen, G. C., Bowden, T. A., & Shi, X. (2021). Recent Advances in Bunyavirus Glycoprotein Research: Precursor Processing, Receptor Binding and Structure. Viruses, 13(2), 353. https://doi.org/10.3390/v13020353

Ikegami, T., Peters, C. J., & Makino, S. (2005). Rift Valley Fever Virus Nonstructural Protein NSs Promotes Viral RNA Replication and Transcription in a Minigenome System. Journal of Virology, 79(9), 5606–5615. https://doi.org/10.1128/jvi.79.9.5606-5615.2005

Jeon, K., Ro, H., Kang, J., Jeong, D., Kim, J., Lee, Y., Yoon, G., Kang, J., Bae, J., Kim, J. I., Park, M., Lee, K. H., Cho, H., Kim, Y., & Cho, N. (2023). A natural variation in the RNA polymerase of severe fever with thrombocytopenia syndrome virus enhances viral replication and in vivo virulence. Journal of Medical Virology, 95(9). https://doi.org/10.1002/jmv.29099

Jiang, X., Zhang, S., Jiang, M., Bi, Z., Liang, M., Ding, S., Wang, S., Liu, J., Zhou, S., Zhang, X., Li, D., & Xu, A. (2015). A cluster of person-to-person transmission cases caused by SFTS virus in Penglai, China. Clinical Microbiology and Infection, 21(3), 274–279. https://doi.org/10.1016/j.cmi.2014.10.006

Lei, X. Y., Liu, M. M., & Yu, X. J. (2015). Severe fever with thrombocytopenia syndrome and its pathogen SFTSV. Microbes and Infection, 17(2), 149–154. https://doi.org/10.1016/j.micinf.2014.12.002

Lin, T., Ou, S., Maeda, K., Shimoda, H., Chan, J. P., Tu, W., Hsu, W., & Chou, C. (2020). The first discovery of severe fever with thrombocytopenia syndrome virus in Taiwan. Emerging Microbes & Infections, 9(1), 148–151. https://doi.org/10.1080/22221751.2019.1710436

Linthicum, K. J., Britch, S. C., & Anyamba, A. (2016). Rift Valley Fever: An Emerging Mosquito-Borne Disease. Annual Review of Entomology, 61(1), 395–415. https://doi.org/10.1146/annurev-ento-010715-023819

Liu, M. M., Lei, X. Y., Yu, H., Zhang, J. Z., & Yu, X. J. (2017). Correlation of cytokine level with the severity of severe fever with thrombocytopenia syndrome. Virology Journal, 14(1). https://doi.org/10.1186/s12985-016-0677-1

Lopez, N., Muller, R., Prehaud, C., & Bouloy, M. (1995). The L protein of Rift Valley fever virus can rescue viral ribonucleoproteins and transcribe synthetic genome-like RNA molecules. Journal of Virology, 69(7), 3972–3979. https://doi.org/10.1128/jvi.69.7.3972-3979.1995

Maes, P., Adkins, S., Alkhovsky, S. V., Avšič-Županc, T., Ballinger, M. J., Bente, D. A., Beer, M., Bergeron, É., Blair, C. D., Briese, T., Buchmeier, M. J., Burt, F. J., Calisher, C. H., Charrel, R. N., Choi, I. R., Clegg, J. C. S., De La Torre, J. C., De Lamballerie, X., DeRisi, J. L., . . . Kuhn, J. H. (2019). Taxonomy of the order Bunyavirales: second update 2018. Archives of Virology, 164(3), 927–941. https://doi.org/10.1007/s00705-018-04127-3

Malet, H., Williams, H. M., Cusack, S., & Rosenthal, M. (2023). The mechanism of genome replication and transcription in bunyaviruses. PLoS Pathogens, 19(1), e1011060. https://doi.org/10.1371/journal.ppat.1011060

Neriya, Y., Kojima, S., Sakiyama, A., Kishimoto, M., Iketani, T., Watanabe, T., Abe, Y., Shimoda, H., Nakagawa, K., Koma, T., & Matsumoto, Y. (2022). A comprehensive list of the Bunyavirales replication promoters reveals a unique promoter structure in Nairoviridae differing from other virus families. Scientific Reports, 12(1). https://doi.org/10.1038/s41598-022-17758-z

Osako, H., Xu, Q., Nabeshima, T., Balingit, J. C., Nwe, K. M., Yu, F., Inoue, S., Hayasaka, D., Tun, M. M. N., Morita, K., & Takamatsu, Y. (2024). Clinical Factors Associated with SFTS Diagnosis and Severity in Cats. Viruses, 16(6), 874. https://doi.org/10.3390/v16060874

Ozawa, M., Victor, S. T., Taft, A. S., Yamada, S., Li, C., Hatta, M., Das, S. C., Takashita, E., Kakugawa, S., Maher, E. A., Neumann, G., & Kawaoka, Y. (2011). Replication-incompetent influenza A viruses that stably express a foreign gene. Journal of General Virology, 92(12), 2879–2888. https://doi.org/10.1099/vir.0.037648-0

Park, S. C., Park, J. Y., Choi, J. Y., Lee, S. G., Eo, S. K., Oem, J. K., Tark, D. S., You, M., Yu, D. H., Chae, J. S., & Kim, B. (2020). Pathogenicity of severe fever with thrombocytopenia syndrome virus in mice regulated in type I interferon

signaling. Laboratory Animal Research, 36(1). https://doi.org/10.1186/s42826-020-00070-0

Park, S. W., Han, M. G., Yun, S. M., Park, C., Lee, W. J., & Ryou, J. (2014). Severe Fever with Thrombocytopenia Syndrome Virus, South Korea, 2013. Emerging Infectious Diseases, 20(11), 1880–1882. https://doi.org/10.3201/eid2011.140888

Ren, F., Shen, S., Wang, Q., Wei, G., Huang, C., Wang, H., Ning, Y., Zhang, D., & Deng, F. (2021). Recent Advances in Bunyavirus Reverse Genetics Research: Systems Development, Applications, and Future Perspectives. Frontiers in Microbiology, 12. https://doi.org/10.3389/fmicb.2021.771934

Ren, Y. T., Tian, H. P., Xu, J. L., Liu, M. Q., Cai, K., Chen, S. L., Ni, X. B., Li, Y. R., Hou, W., & Chen, L. J. (2023). Extensive genetic diversity of severe fever with thrombocytopenia syndrome virus circulating in Hubei Province, China, 2018–2022. PLoS Neglected Tropical Diseases, 17(9), e0011654. https://doi.org/10.1371/journal.pntd.0011654

Robles, N. J. C., Han, H. J., Park, S. J., & Choi, Y. K. (2018). Epidemiology of severe fever and thrombocytopenia syndrome virus infection and the need for therapeutics for the prevention. Clinical and Experimental Vaccine Research, 7(1), 43. https://doi.org/10.7774/cevr.2018.7.1.43

Šali, A., & Blundell, T. L. (1993). Comparative Protein Modelling by Satisfaction of Spatial Restraints. Journal of Molecular Biology, 234(3), 779–815. https://doi.org/10.1006/jmbi.1993.1626

Sansilapin, C., Tangwangvivat, R., Hoffmann, C. S., Chailek, C., Lekcharoen, P., Thippamom, N., Petcharat, S., Taweethavonsawat, P., Wacharapluesadee, S., Buathong, R., Kurosu, T., Yoshikawa, T., Shimojima, M., Iamsirithaworn, S., & Putcharoen, O. (2024). Severe fever with thrombocytopenia syndrome (SFTS) in Thailand: using a one health approach to respond to novel zoonosis and its implications in clinical practice. One Health Outlook, 6(1). https://doi.org/10.1186/s42522-024-00112-w

Shimada, S., Aoki, K., Nabeshima, T., Fuxun, Y., Kurosaki, Y., Shiogama, K., Onouchi, T., Sakaguchi, M., Fuchigami, T., Ono, H., Nishi, K., Posadas-Herrera, G., Uchida, L., Takamatsu, Y., Yasuda, J., Tsutsumi, Y., Fujita, H., Morita, K., & Hayasaka, D. (2016). Tofla virus: A newly identified Nairovirus of the Crimean-Congo hemorrhagic fever group isolated from ticks in Japan. Scientific Reports, 6(1). https://doi.org/10.1038/srep20213

Shimada, S., Posadas-Herrera, G., Aoki, K., Morita, K., & Hayasaka, D. (2015). Therapeutic effect of post-exposure treatment with antiserum on severe fever with thrombocytopenia syndrome (SFTS) in a mouse model of SFTS virus infection. Virology, 482, 19–27. https://doi.org/10.1016/j.virol.2015.03.010

Shimojima, M., Sugimoto, S., Taniguchi, S., Maeki, T., Yoshikawa, T., Kurosu, T., Tajima, S., Lim, C. K., & Ebihara, H. (2024). N-glycosylation of viral glycoprotein is a novel determinant for the tropism and virulence of highly

pathogenic tick-borne bunyaviruses. PLoS Pathogens, 20(7), e1012348. https://doi.org/10.1371/journal.ppat.1012348

Simons, J. F., & Pettersson, R. F. (1991). Host-derived 5' ends and overlapping complementary 3' ends of the two mRNAs transcribed from the ambisense S segment of Uukuniemi virus. Journal of Virology, 65(9), 4741–4748. https://doi.org/10.1128/jvi.65.9.4741-4748.1991

Smithburn, K. C., Haddow, A. J., & Mahaffy, A. F. (1946). A neurotropic virus isolated from Aedes mosquitoes caught in the Semliki forest: A neurotropic virus isolated from Aedes mosquitoes caught in the Semliki forest. The American Journal of Tropical Medicine and Hygiene, s1-26(2), 189–208. https://doi.org/10.4269/ajtmh.1946.s1-26.189

Sun, Y., Li, J., Gao, G. F., Tien, P., & Liu, W. (2018). Bunyavirales ribonucleoproteins: the viral replication and transcription machinery. Critical Reviews in Microbiology, 44(5), 522–540. https://doi.org/10.1080/1040841x.2018.1446901

Takahashi, T., Maeda, K., Suzuki, T., Ishido, A., Shigeoka, T., Tominaga, T., Kamei, T., Honda, M., Ninomiya, D., Sakai, T., Senba, T., Kaneyuki, S., Sakaguchi, S., Satoh, A., Hosokawa, T., Kawabe, Y., Kurihara, S., Izumikawa, K., Kohno, S., . . . Saijo, M. (2013a). The First Identification and Retrospective Study of Severe Fever With Thrombocytopenia Syndrome in Japan. The Journal of Infectious Diseases, 209(6), 816–827. https://doi.org/10.1093/infdis/jit603

Tang, X., Wu, W., Wang, H., Du, Y., Liu, L., Kang, K., Huang, X., Ma, H., Mu, F., Zhang, S., Zhao, G., Cui, N., Zhu, B. P., You, A., Chen, H., Liu, G., Chen, W., & Xu, B. (2012). Human-to-Human Transmission of Severe Fever With Thrombocytopenia Syndrome Bunyavirus Through Contact With Infectious Blood. The Journal of Infectious Diseases, 207(5), 736–739. https://doi.org/10.1093/infdis/jis748

Tercero, B., & Makino, S. (2020). Reverse genetics approaches for the development of bunyavirus vaccines. Current Opinion in Virology, 44, 16–25. https://doi.org/10.1016/j.coviro.2020.05.004

Tran, X. C., Yun, Y., Van An, L., Kim, S. H., Thao, N. T. P., Man, P. K. C., Yoo, J. R., Heo, S. T., Cho, N. H., & Lee, K. H. (2019). Endemic Severe Fever with Thrombocytopenia Syndrome, Vietnam. Emerging Infectious Diseases, 25(5), 1029–1031. https://doi.org/10.3201/eid2505.181463

Wulandari, S., Nyampong, S., Lokupathirage, S. M. W., Yoshimatsu, K., Shimoda, H., & Hayasaka, D. (2024). Development of an Entirely Cloned cDNA-Based Reverse Genetics System for Tofla Virus of Orthonairovirus. Virology, 110170. https://doi.org/10.1016/j.virol.2024.110170

Xing, X., Guan, X., Liu, L., Xu, J., Li, G., Zhan, J., Liu, G., Jiang, X., Shen, X., Jiang, Y., Wu, Y., Zhang, H., Huang, J., Ding, F., Sha, S., Liu, M., & Zhan, F. (2017). A Case-control Study of Risk Sources for Severe Fever with Thrombocytopenia

Syndrome in Hubei Province, China. International Journal of Infectious Diseases, 55, 86–91. https://doi.org/10.1016/j.ijid.2017.01.003

Yamanaka, A., Kirino, Y., Fujimoto, S., Ueda, N., Himeji, D., Miura, M., Sudaryatma, P. E., Sato, Y., Tanaka, H., Mekata, H., & Okabayashi, T. (2020). Direct Transmission of Severe Fever with Thrombocytopenia Syndrome Virus from Domestic Cat to Veterinary Personnel. Emerging Infectious Diseases, 26(12), 2994–2998. https://doi.org/10.3201/eid2612.191513

Ye, W., & Yan, F. (2024). Editorial: Bunyaviruses - threats to health and economy. Frontiers in Cellular and Infection Microbiology, 14. https://doi.org/10.3389/fcimb.2024.1369530

Yoshikawa, R., Kawakami, M., & Yasuda, J. (2023). The NSs protein of severe fever with thrombocytopenia syndrome virus differentially inhibits the type 1 interferon response among animal species. Journal of Biological Chemistry, 299(6), 104819. https://doi.org/10.1016/j.jbc.2023.104819

Yu, K. M., Park, S. J., Yu, M. A., Kim, Y. I., Choi, Y., Jung, J. U., Brennan, B., & Choi, Y. K. (2019). Cross-genotype protection of live-attenuated vaccine candidate for severe fever with thrombocytopenia syndrome virus in a ferret model. Proceedings of the National Academy of Sciences, 116(52), 26900–26908. https://doi.org/10.1073/pnas.1914704116

Yu, L., Zhang, L., Sun, L., Lu, J., Wu, W., Li, C., Zhang, Q., Zhang, F., Jin, C., Wang, X., Bi, Z., Li, D., & Liang, M. (2012). Critical Epitopes in the Nucleocapsid Protein of SFTS Virus Recognized by a Panel of SFTS Patients Derived Human Monoclonal Antibodies. PLoS ONE, 7(6), e38291. https://doi.org/10.1371/journal.pone.0038291

Yu, X., Liang, M., Zhang, S., Liu, Y., Li, J., Sun, Y., Zhang, L., Zhang, Q., Popov, V. L., Li, C., Qu, J., Li, Q., Zhang, Y., Hai, R., Wu, W., Wang, Q., Zhan, F., Wang, X., Kan, B., . . . Li, D. (2011). Fever with Thrombocytopenia Associated with a Novel Bunyavirus in China. New England Journal of Medicine, 364(16), 1523–1532. https://doi.org/10.1056/nejmoa1010095

Yun, S., Park, S., Kim, Y., Park, S., Yu, M., Kwon, H., Kim, E., Yu, K., Jeong, H. W., Ryou, J., Lee, W., Jee, Y., Lee, J., & Choi, Y. K. (2019). Genetic and pathogenic diversity of severe fever with thrombocytopenia syndrome virus (SFTSV) in South Korea. JCI Insight, 5(2). https://doi.org/10.1172/jci.insight.129531

Zhang, X., Ma, Y., Zhang, Y., Hu, Z., Zhang, J., Han, S., Wang, G., Li, S., Wang, X., Tang, F., Liang, W., Yuan, H., Zhao, J., Jiang, L., Zhang, L., Si, G., Peng, C., Wang, R., Ge, H., . . . Liu, W. (2024). A New Orthonairovirus Associated with Human Febrile Illness. New England Journal of Medicine, 391(9), 821–831. https://doi.org/10.1056/nejmoa2313722